Organic & Biomolecular Chemistry

PAPER

View Article Online
View Journal | View Issue

Cite this: *Org. Biomol. Chem.*, 2016, **14**, 10599

Effect of novel triazole–amino acid hybrids on growth and virulence of *Candida* species: *in vitro* and *in vivo* studies†

Babita Aneja,‡[a,b] Mohammad Irfan,‡[a,c] Charu Kapil,[d] Mohamad Aman Jairajpuri,[d] Ronan Maguire,[e] Kevin Kavanagh,[e] M. Moshahid A. Rizvi,[f] Nikhat Manzoor,*§[c] Amir Azam[b] and Mohammad Abid*¶[a]

Received 8th August 2016,
Accepted 5th October 2016

DOI: 10.1039/c6ob01718e

www.rsc.org/obc

The increasing incidence of human candidiasis and the tendency of *Candida* species to become resistant to existing chemotherapies are well-recognized health problems. The present study demonstrates the successful synthesis of novel triazole–amino acid hybrids with potent *in vitro* and *in vivo* inhibitory activity against *Candida* species. Particularly, compounds **68** and **70** showed potent *in vitro* activity against fluconazole (FLC) resistant as well as sensitive clinical isolates of *Candida albicans*. Time kill curve analysis of lead inhibitors **68** and **70** showed their fungistatic nature. Secretion of hydrolytic enzymes, mainly proteinases and phospholipases, decreased considerably in the presence of **68** and **70** indicating their interference in fungal virulence. TEM analysis of *Candida* cells exposed to compounds **68** and **70** clearly showed morphological changes and intracellular damage as their possible mode of action. A preliminary mechanistic study carried out on the two most effective inhibitors (**68** and **70**) revealed the inhibition of ergosterol biosynthesis thereby causing the cells to lose their integrity and viability. The selected compounds did not show significant cytotoxicity up to a concentration of 200 μg mL^{-1} in the HEK293 cell line. An *in silico* analysis of **68** and **70** binding to a modeled *C. albicans* CYP51 showed critical H-bonding as well as hydrophobic interactions with the important active site residues indicating the basis of their anti-*Candida* role. Studies on the larvae of *Galleria mellonella* showed that the selected inhibitors (**68** and **70**) were non-toxic, did not provoke an immune response and significantly reduced *Candida* proliferation *in vivo*.

Introduction

Over the past three decades, the frequency of fungal infections in humans has increased dramatically worldwide despite the extensive efforts towards the discovery of novel antifungal agents and the availability of various drugs.[1–3] Of particular concern is the severity associated with the ever-increasing incidences of hospital-acquired systemic mycoses, caused by various species of *Candida*, responsible for the crude mortality rate of up to 50% in the United States alone.[4] Adding to this disease burden, superficial infections of skin and nails in humans are affecting ~25% of the general population worldwide.[5] It has been reported that the use of broad-spectrum antibiotics, suppression of immune response during organ and bone marrow transplantation, cancer treatment and AIDS are increasing the chances of *Candida* infections thus further aggravating the condition.[6] Among many *Candida* species, *C. albicans* is a prominent *Candida* species which is responsible for a major cause of candidiasis and isolated from approximately 80% of cases of candidemia.[7] However, the

[a]*Medicinal Chemistry Lab, Department of Biosciences, Jamia Millia Islamia (A Central University), Jamia Nagar, New Delhi 110025, India. E-mail: mabid@jmi.ac.in; Fax: +91-11-26980229; Tel: +91-8750295095*
[b]*Department of Chemistry, Jamia Millia Islamia (A Central University), Jamia Nagar, New Delhi 110025, India*
[c]*Medical Mycology Lab, Department of Biosciences, Jamia Millia Islamia (A Central University), Jamia Nagar, New Delhi 110025, India. E-mail: nmanzoor@jmi.ac.in*
[d]*Protein Conformation and Enzymology Lab, Department of Biosciences, Jamia Millia Islamia (A Central University), Jamia Nagar, New Delhi 110025, India*
[e]*Department of Biology, Maynooth University, Co. Kildare, Ireland*
[f]*Genome Biology Lab, Department of Biosciences, Jamia Millia Islamia (A Central University), Jamia Nagar, New Delhi 110025, India*

†Electronic supplementary information (ESI) available. See DOI: 10.1039/c6ob01718e

‡These authors contributed equally to this work.

§Present address: College of Applied Medical Sciences, Taibah University, Al-Madinah Al-Munawarah, KSA.

¶Present address: Eppley Institute for Research in Cancer and Allied Diseases, University of Nebraska Medical Center, Omaha, NE 68198-6805, USA.

number of infections caused by other non-*Candida albicans Candida* species (NCAC) which include *C. glabrata*, *C. tropicalis* and *C. parapsilosis* has also increased.[8]

During both superficial and systemic infection, pathogenicity of *Candida* species relies on a number of virulence factors including the capability to adhere onto the surface that assists them to colonize the host. Adhesion is mainly influenced by the profile of cell wall proteins and cell surface physicochemical properties.[9] In addition to this, they also adhere to the surface of medical devices and form biofilms which limit the penetration of substances through the matrix and decrease the susceptibility of *Candida* to antifungal therapy.[10] *Candida* also secrete different hydrolytic enzymes like proteinases, phospholipases and hemolysins and acquire nutrients and disseminate within the host. They also modulate the host immune response and cause destruction of host tissues.[11]

Treatment of *Candida* infections relies on a limited number of chemotherapeutic agents including polyenes, azoles, echinocandins, allylamines and flucytosine.[12] Among them, azoles such as fluconazole (FLC), itraconazole, voriconazole, posaconazole, ketoconazole, miconazole and econazole (Fig. 1) are widely used for the treatment of both superficial and invasive fungal infections due to their favourable pharmacokinetics and safety profile.[6] Azoles target the biosynthesis of ergosterol, a major component of the fungal membrane, by inhibiting the cytochrome P450-dependent enzyme lanosterol 14α-demethylase (CYP51). The depletion of ergosterol and accumulation of toxic methylsterols in the membrane result in the alteration of membrane fluidity along with disruption of activity of membrane-bound enzymes leading to the inhibition of fungal growth and replication.[13] Although azoles have an advantage of oral administration, they lack fungicidal effects as well as possess limited selectivity for fungal demethylase enzyme over mammalian cytochrome P450s thus posing serious side effects.[14] Moreover, the increased use of azole antifungals has contributed to the emerging resistance in *Candida* species which is prompting the medicinal chemists worldwide to develop novel and more effective antifungal agents with a broad spectrum, better pharmacokinetic profile and low toxicity.[15]

Previously, it was reported that triazole–amino acids clubbed with an indole moiety have potent antifungal effects as they caused detrimental effects on the sterol biosynthetic pathway of *C. albicans* thus inducing cell wall defects leading to cell death in combination with currently available azole antifungals.[16] On the basis of these findings on triazole–amino acid scaffolds and in continuation of our efforts for the development of antimicrobial agents,[17–19] we report herein the synthesis of a series of novel triazole–amino acid hybrids (**65–88**) and their screening against three species of *Candida* (*C. albicans*, *C. glabrata* and *C. tropicalis*). This leads to the identification of 1,2,3-triazoles bearing phenylalanine (**68**) and tryptophan tails (**70**) as potent antifungals against FLC sensitive and resistant clinical isolates of *C. albicans*. Moreover, compounds with comparatively lower IC_{50} values were also subjected to cell proliferation assay on the HEK293 (Human Embryonic Kidney) cell line and were found to be non-toxic up to a 200 μg mL^{-1} concentration. Various assays for growth (time kill curve) and virulence (proteinase and phospholipase secretion) performed on *Candida* cells exposed to lead inhibitors (**68** and **70**) also showed promising results. A detailed study of lead compounds (**68** and **70**) on the larvae of *Galleria mellonella* further confirmed their non-toxic behavior and a significant reduction in *Candida* proliferation *in vivo*. Because of the importance of CYP51 in the antifungal drug studies, molecular docking was performed for the most active compounds against the predicted three-dimensional model of CYP51 from *C. albicans* in order to shed light on the mechanism and plausible binding modes of the compounds to the target enzyme. Our study revealed that the triazole–amino acid hybrids (**68** and **70**) provide a suitable core to be exploited for lead optimization to develop potent antifungal agents.

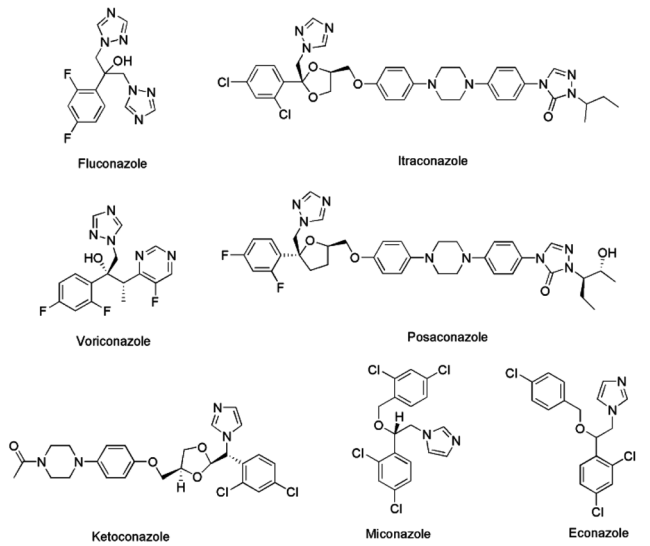

Fig. 1 Structure of common azole-based antifungal drugs.

Results and discussion

Chemistry

The multistep synthetic approach was adopted for the preparation of the title compounds (**65–88**) as given in Scheme 1. Substituted benzylamines (**17–24**) were obtained *via* a two-step sequence involving oximation of substituted aryl aldehydes (**1–8**) followed by Zn/HCl mediated reduction.[18] Then, in another set of reactions azidopropionic acid, **26**, was obtained from 3-bromopropionic acid, **25**, by direct azide replacement using sodium azide in anhyd. DMF at 85 °C. Coupling of azidopropionic acid, **26**, with substituted benzylamines **17–24** in the presence of 1-ethyl-3-(3-dimethylaminopropyl) carbodiimide (EDC·HCl) and 1-hydroxybenzotriazole (HOBt) in acetonitrile yielded the corresponding azide intermediates **27–34** in moderate yield. In a separate set of reactions, boc-protected L-amino acids (**35–37**) were treated with propargyl bromide in

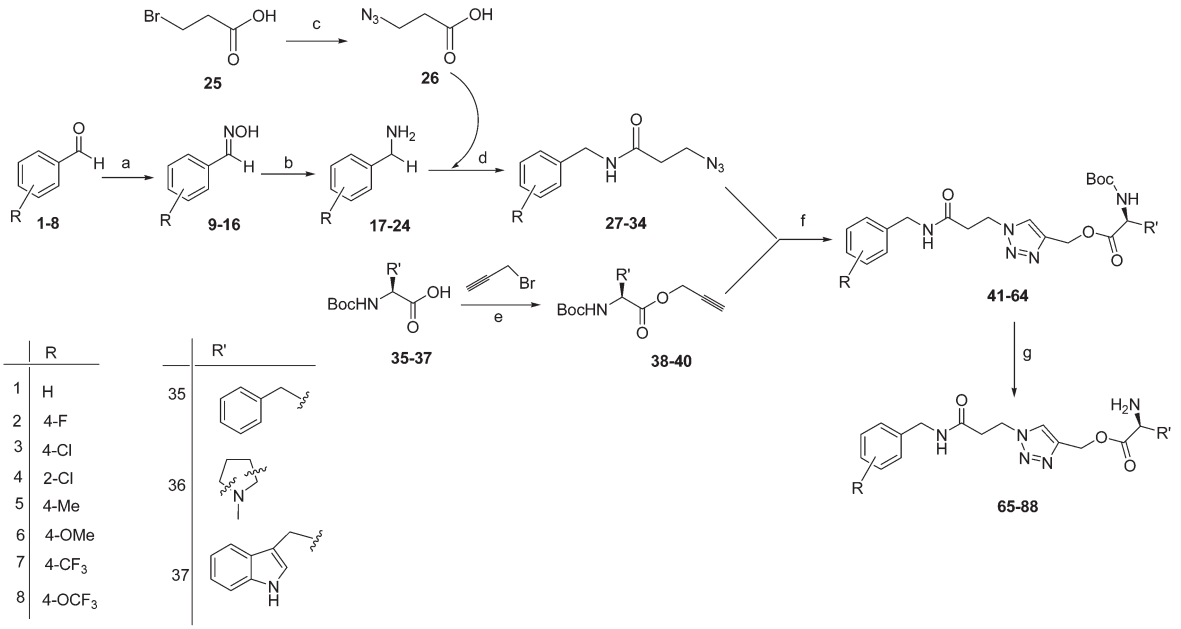

Scheme 1 Synthesis of triazole–amino acid hybrids. Reagents and conditions (a) $NH_2OH{\cdot}HCl$, pyridine/ethanol (1 : 10), reflux; (b) Zn, HCl, ethanol, rt; (c) NaN_3, DMF, reflux; (d) HOBt, EDC·HCl, NMM, CH_3CN, rt; (e) propargyl bromide, K_2CO_3, DMF, rt; (f) $CuSO_4{\cdot}5H_2O$, sodium ascorbate, *tert*-butanol : water (1 : 2), rt; (g) *p*TSA, DCM, rt.

the presence of K_2CO_3 to provide alkyne intermediates (**39–40**) in excellent yield. Finally, the 1,2,3-triazole–amino acid hybrids (**41–64**) were synthesized *via* the Huisgen 1,3-dipolar cycloaddition reaction between alkynes **39–40** and azides **27–34** in the presence of copper sulphate and sodium ascorbate in a *tert*-butanol : water (1 : 2) mixture. The key intermediates, **41–64** were finally deprotected utilizing *p*-toluenesulfonic acid in dichloromethane to yield title compounds **65–88** in high yield (Table 1).

In vitro anti-*Candida* activity

We generated a library of 24 compounds that features the 1,2,3-triazole core and an amino acid (Phe/Pro/Trp) as a tail and screened all the analogues for *in vitro* anticandidal activity. Preliminary studies were done on three different *Candida* species: *C. albicans*, *C. glabrata* and *C. tropicalis* to see the effect of these analogues on the growth of *Candida* cells *in vitro* (Table 2). Fluconazole was used as a positive control. The unsubstituted and *para*-halogen substituted benzyl compounds with an L-phenylalanine tail showed modest activity (70.9–179.4 μg mL^{-1}) against most pathogenic *C. albicans* ATCC 90028 strain. Compound **68** with *p*-fluoro substitution and a phenylalanine tail emerged as the most potent (IC_{50} = 70.9 μg mL^{-1}) among all in the series as a selective inhibitor of *C. albicans* ATCC 90028 strain. Chloro substitution at the *ortho* position to the benzyl group (**74**) resulted in the decrease of activity (340.0 μg mL^{-1}) in the same strain. The structure-activity relationship could not be established clearly in the case of analogues with an L-proline tail. Moreover, compound **66** bearing an unsubstituted benzyl group and an L-proline tail exhibited an IC_{50} value of 203.5 μg mL^{-1} in *C. glabrata* ATCC 90030 strain. It was found that the unsubstituted and *para*-substituted triazole analogues with a tryptophan tail showed the best anticandidal activity against *C. albicans* ATCC 90028 strain. Compound **70** with *p*-fluoro substitution emerged as the most potent anticandidal agent (IC_{50} = 22.4 μg mL^{-1}) compared to **67**, with no substitution, having IC_{50} = 98.8 μg mL^{-1} against *C. albicans* ATCC 90028 strain. It also inhibited the growth of *C. glabrata* with an IC_{50} of 163.2 μg mL^{-1}. The *p*-methyl (**79**, IC_{50} = 168.7 μg mL^{-1}) and *p*-methoxy (**82**, IC_{50} = 163.9 μg mL^{-1}) substitution were well tolerated compared to *p*-trifluoromethyl (**85**, IC_{50} = 282.6 μg mL^{-1}) and *p*-trifluoromethoxy (**88**, IC_{50} = 1142.7 μg mL^{-1}) substitution where the activity was completely lost against *C. albicans* ATCC 90028 strain. Based on the results obtained with standard *Candida* strains, seven compounds (**67**, **68**, **70**, **71**, **73**, **79** and **82**) were selected for further investigation against both FLC-sensitive and resistant clinical *C. albicans* strains. Compounds with *p*-fluoro substitution with phenylalanine (**68**) and tryptophan (**70**) tails emerged as the most potent inhibitors for clinical strains too. Compound **68** showed a moderate inhibitory effect on clinically isolated *C. albicans* with IC_{50} in the range of 154.9–188.3 μg mL^{-1}. Similarly, compound **70** also showed inhibition of clinically isolated *Candida* cells with IC_{50} in the range of 149.63–176.1 μg mL^{-1}. Both compounds, **68** and **70** showed potent inhibitory activity against FLC-resistant *C. albicans* with IC_{50} values of 671.08 and 634.98 μg mL^{-1}, respectively, which otherwise is tolerant to FLC (IC_{50} > 1000 μg mL^{-1}) (Table 3). The results prompted us to further explore the effect of these two lead inhibitors (**68** and **70**) on the growth of *Candida* sp. The fungistatic or fungicidal nature of lead compounds (**68** and **70**) was determined by time kill curve studies

Table 1 Structure of triazole–amino acid hybrids

Benzylamine	L-Phenylalanine	L-Proline	L-Tryptophan
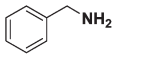	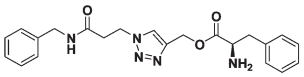 65	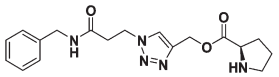 66	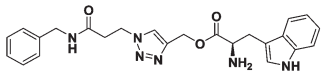 67
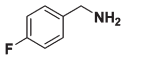	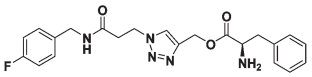 68	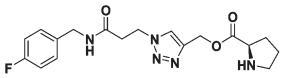 69	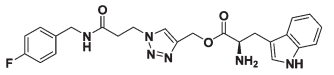 70
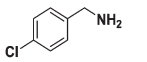	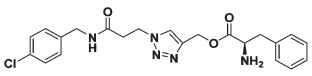 71	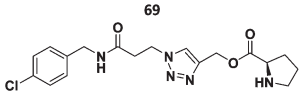 72	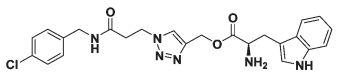 73
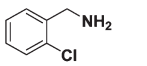	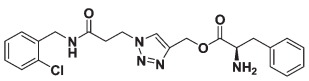 74	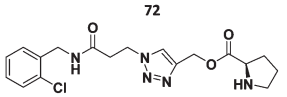 75	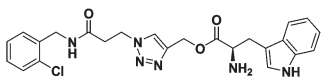 76
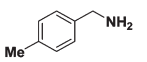	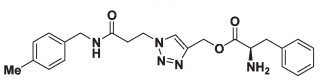 77	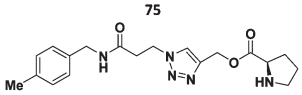 78	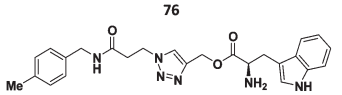 79
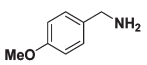	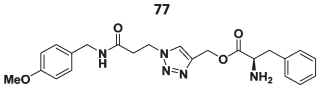 80	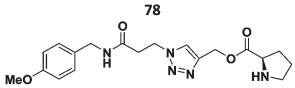 81	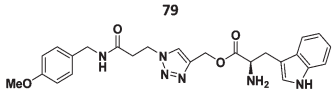 82
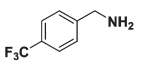	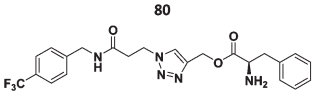 83	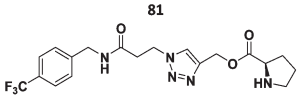 84	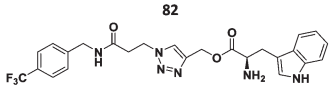 85
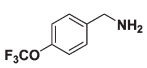	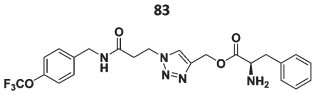 86	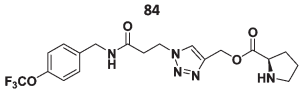 87	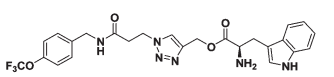 88

Table 2 *In vitro* anticandidal activity of compounds **65–88** (IC_{50} in μg mL^{-1}) against standard strains of *Candida*

Comp.	*C. alb.*	*C. gla.*	*C. tro.*	^{1}*C. alb.*
65	179.4	506.5	364.7	377.0
66	473.8	203.5	741.5	541.3
67	98.8	944.1	475.7	303.7
68	70.9	1352.0	503.0	335.6
69	326.3	912.2	678.9	369.3
70	22.4	163.2	349.0	269.5
71	164.1	1065.3	389.4	314.9
72	420.2	267.4	927.1	351.8
73	161.0	975.5	556.4	313.3
74	340.0	383.6	421.4	303.5
75	376.0	247.5	852.0	333.8
76	227.1	684.3	542.3	378.7
77	294.4	851.3	497.7	300.3
78	478.7	326.9	684.3	636.5
79	168.7	1074.0	618.3	379.0
80	300.2	1121.1	447.8	292.7
81	554.0	265.6	571.2	562.3
82	163.9	427.2	423.6	340.9
83	315.3	371.1	407.6	310.0
84	526.0	268.3	468.0	580.3
85	282.6	272.4	662.3	321.3
86	865.4	1103.7	923.8	747.2
87	985.0	1006.4	971.4	966.0
88	1142.7	1081.6	991.0	998.8
FLC	15.6	7.8	8.5	n.d.

Abbreviations: *C. alb.* = C. *albicans* ATCC 90028; *C. gla.* = *C. glabrata* ATCC 90030; *C. tro.* = *C. tropicalis* ATCC 750; ^{1}*C. alb.* = *C. albicans* ATCC 1026; n.d. = not done; NA = not active; FLC = fluconazole.

Table 3 *In vitro* anticandidal activity of selected potential compounds against clinical isolate of *C. albicans*

Compound	**C. alb.*	**C. alb.*	**C. alb.*	†*C. alb.*
67	192.86	343.63	322.05	>1000
68	154.92	188.37	183.13	671.08
70	149.63	153.19	176.10	634.98
71	387.90	206.48	368.69	>1000
73	237.52	358.43	344.70	>1000
79	563.93	249.64	258.77	>1000
82	297.62	199.52	341.76	>1000
FLC	<7.81	<7.81	<7.81	>1000

Abbreviations: **C. alb.* = *C. albicans* (fluconazole sensitive); †*C. alb.* = *C. albicans* (fluconazole resistant).

on FLC-sensitive as well as resistant strains of *C. albicans*. Both compounds showed a fungistatic effect on the growth of *C. albicans* with an efficacy much superior to that of the conventional standard drug fluconazole. Furthermore, no significant changes in growth were observed at the concentrations lower than 120 μg mL^{-1} of compounds **68** and **70** (Fig. 2).

Extracellular hydrolytic enzymes (*e.g.* phospholipases and proteinases) are potent virulence factors which play an important role in the establishment of *Candida* infection.[20] To investigate whether the lead compounds (**68** and **70**) have any effect on the extracellular secretion of these enzymes, an inhibition

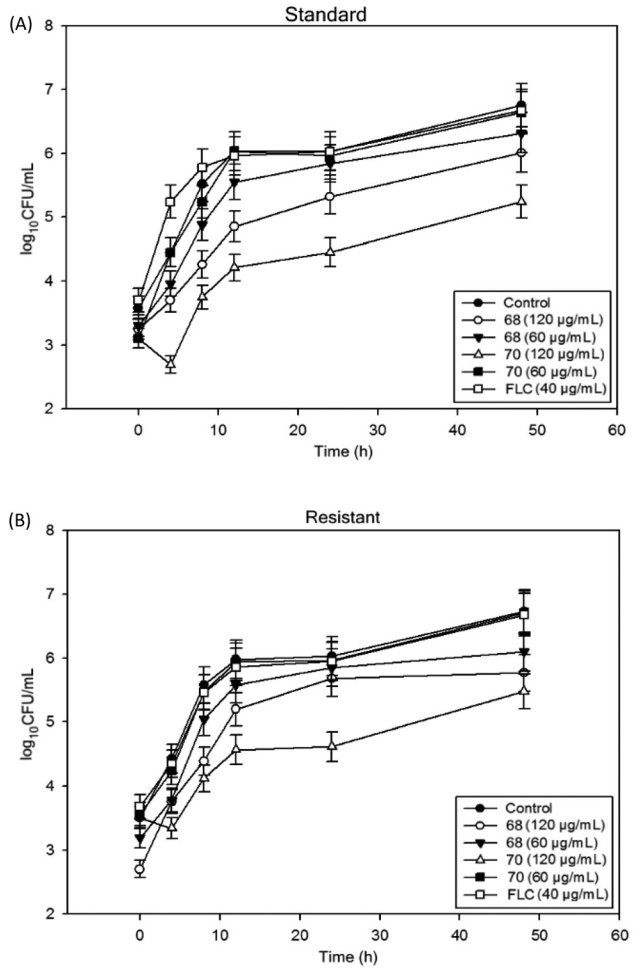

Fig. 2 Time kill curves of (A) fluconazole sensitive *C. albicans* ATCC 90028; (B) fluconazole resistant *C. albicans* at various concentrations of **68** and **70**. The results indicate the fungi-static nature of these compounds.

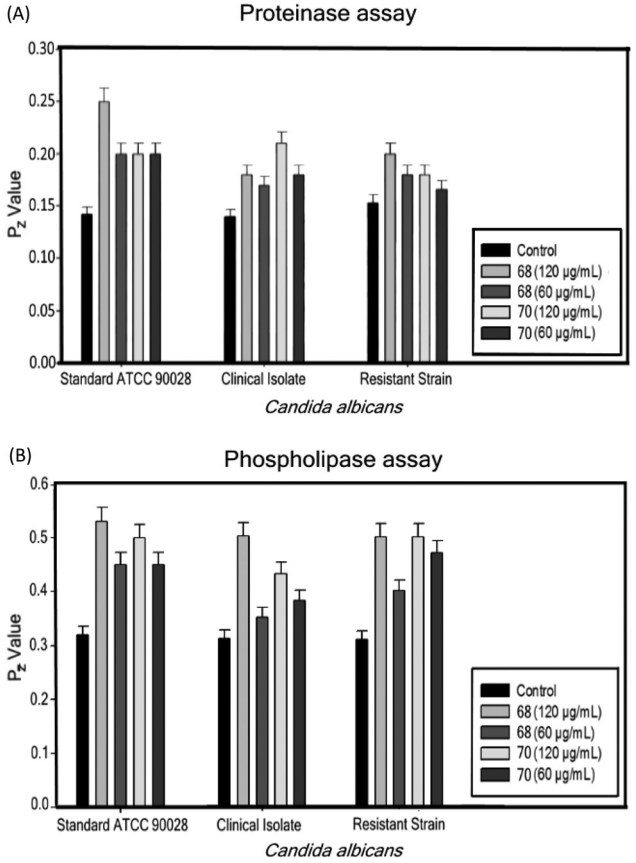

Fig. 3 Effect of compounds **68** and **70** on (A) proteinase secretion and; (B) phospholipase secretion. These hydrolytic enzymes act as a potent virulence factor and play an important role in the establishment of *Candida* infection. The higher P_z value indicates the lower secretion of enzyme. At a 125 μg mL^{-1} concentration, compounds **68** and **70** cause 17 to 38% decrease in secretion of these enzymes.

assay was performed using standard as well as resistant *C. albicans* strains. The results showed that on treatment with 120 μg mL^{-1} of compound **68**, proteinase secretion was decreased by 29, 22 and 23.5% in standard, FLC-sensitive and resistant strains of *C. albicans*, respectively, while at the same concentration, compound **70** decreased the proteinase secretion by 30, 33 and 17% against the respective strains. Similar results were obtained at a 60 μg mL^{-1} concentration of both compounds, **68** and **70**, with no significant differences in the inhibition of proteinase secretion (Fig. 3A). At similar concentrations, compound **68** caused 40, 38, and 38% inhibition in phopholipase secretion whereas compound **70** decreased the secretions respectively by 36, 27 and 38% in standard, FLC-sensitive and resistant strains of *C. albicans* (Fig. 3B). Our results suggest that both compounds (**68** and **70**) significantly reduce the secretion of proteinases and phospholipases in *Candida* spp. which are vital to fungal invasion of host tissues and immunosuppression.

The effect of lead compounds (**68** and **70**) on the morphology of *C. albicans* was monitored by transmission electron microscopy (TEM) which led to the exploration of the possible antifungal mechanism of action. *Candida* cells treated with 120 μg mL^{-1} of **68** and **70** and the untreated control cells were used for TEM analysis. It was observed, as shown in Fig. 4,

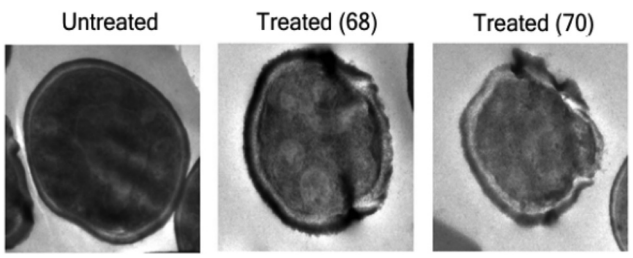

Fig. 4 Representative transmission electron micrographs of *C. albicans* ATCC 90028 cells exposed to **68** and **70** at their respective MICs. The figure showed significant damage to *Candida* cells. The shape of the cell became abnormal and the cell wall lost its integrity, became irregular and ruptured.

that the untreated cells are normal in shape with uniform cell density and an intact cell wall while the treated cells showed several deformations. On exposure to **68** or **70**, significant damage could be seen in *Candida* cells wherein the cell shape became abnormal and the cell wall lost its integrity becoming irregular and ruptured. The intracellular organelles disappeared indicating the necrotic mode of cell death. Thus, we can conclude from the results of TEM analysis that the lead compounds (**68** and **70**) may be interfering with the biosynthesis of the cell membrane.

It is well known that azole drugs like FLC inhibit ergosterol biosynthesis by destroying both membrane integrity and the function of some membrane-bound proteins and therefore affecting fungal cell growth and proliferation.[21] The effect of the lead compounds (**68** and **70**) was studied on ergosterol biosynthesis in *C. albicans* to further support our suggestion that these compounds interfere with the biosynthesis of the cell membrane. The ergosterol content of the exposed cells was estimated in FLC-sensitive and resistant *Candida* cells by a method reported previously by Arthington-Skaggs *et al.*[22] and FLC was used as a positive control. The results showed a dose dependent decrease in the ergosterol content when the cells were grown in varying concentrations of **68** and **70** (Fig. 5). The mean decrease in the total ergosterol content for standard strains was found to be 5% at 30 μg mL^{-1}, 27% at 60 μg mL^{-1} and 73% at 120 μg mL^{-1} of compound **68**. The mean decrease in the total ergosterol content for FLC-resistant *C. albicans* was found to be 2% at 30 μg mL^{-1}, 23% at 60 μg mL^{-1} and 79% at 120 μg mL^{-1} of compound **68**. Similarly, the mean decrease in the total ergosterol content for standard *C. albicans* was found to be 15% at 30 μg mL^{-1}, 37% at 60 μg mL^{-1} and 48% at 120 μg mL^{-1} of **70**. However, the decrease in the total ergosterol content for FLC-resistant *C. albicans* was 7% at 30 μg mL^{-1}, 80% at 60 μg mL^{-1} and 91% at 120 μg mL^{-1} of **70**. In the presence of 100 μg mL^{-1} of FLC, the decrease in the ergosterol content was 25% and 28%, respectively, for standard and FLC-resistant *C. albicans* (Fig. 5). Our results suggest that compounds **68** and **70** inhibit the total ergosterol content more effectively in comparison to FLC in all the *Candida* strains tested here. In conclusion, the lead compounds (**68** and **70**) caused ergosterol depletion resulting in the disruption of the cell membrane which is consistent with the results of TEM analysis.

The cytotoxicity of the compounds with comparatively lower IC_{50} values (**65**, **67–71**, **73–74**, **79**, **82–83**, **85**) was checked by the MTT assay using the HEK293 cell line (Fig. 6). It is evident from the results that all the twelve selected compounds (**65**, **67–71**, **73–74**, **79**, **82–83**, **85**) displayed more than 85% cell viability at 50 μg mL^{-1} concentration. Out of 12, eight compounds (**67–71**, **73**, **79**, **82–83**) displayed more than 70% cell viability even at a concentration of 200 μg mL^{-1} which indicated the non-cytotoxic nature of these compounds. On increasing the concentration from 400 to 600 μg mL^{-1} for all the selected compounds, the cells were found to be more than 50% viable. The hemolytic assay was also performed with lead inhibitors **68** and **70** to exclude any possible toxicity on human RBCs. At 125 μg mL^{-1}, compounds **68** and **70** caused 10% and 15% cell lysis, respectively, in comparison to 36% cell lysis caused by FLC at the same concentration (Fig. 7). More interestingly, compounds **68** and **70** were found negligibly toxic up to 500 μg mL^{-1}, with only 18% and 22% cell lysis, respectively.

Modeling and *in silico* docking

The lanosterol 14-α demethylase enzyme (CYP51) is a member of the cytochrome P450 superfamily which catalyses the

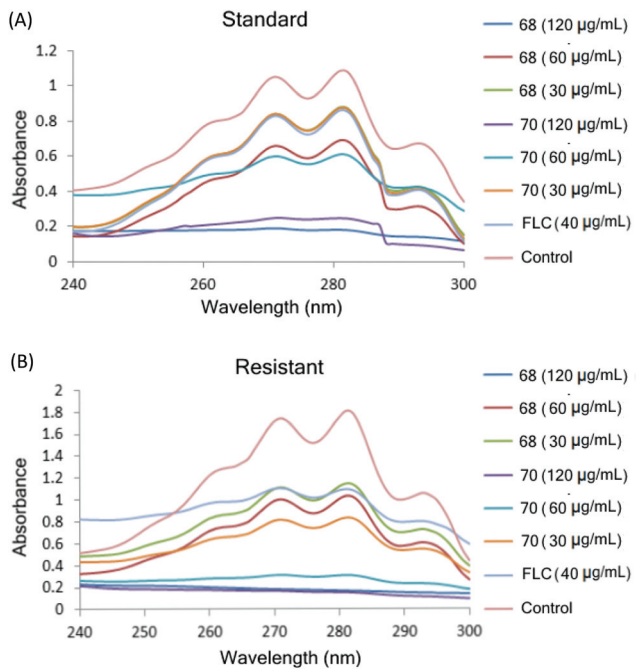

Fig. 5 UV spectrophotometric sterol profiles of (A) fluconazole sensitive standard *C. albicans* ATCC 90028 and; (B) fluconazole resistant *C. albicans*. At 120 μg mL^{-1}, the mean decrease in total ergosterol content for standard as well as resistant *C. albicans* were found in the range of 48–96%.

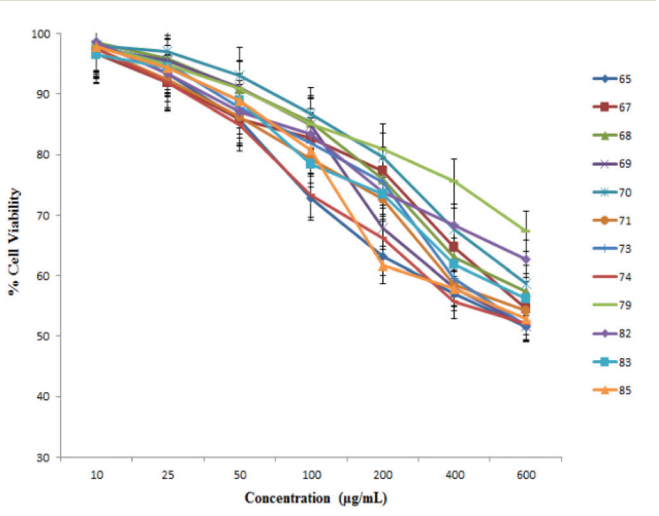

Fig. 6 Cell viability assay on the HEK293 cell line.

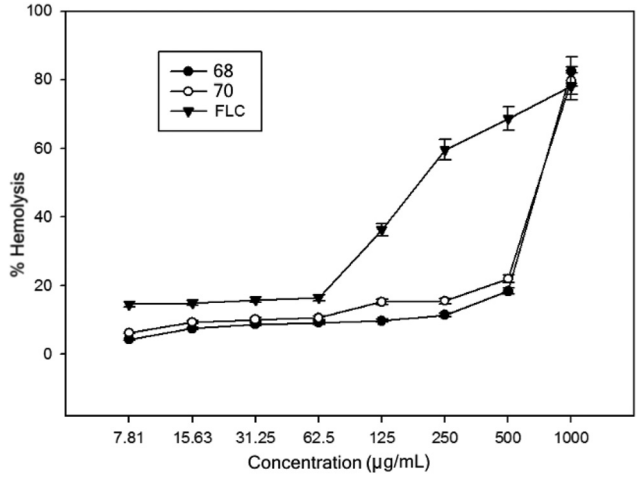

Fig. 7 Hemolytic assay for compounds **68** and **70** on human red blood cells (hRBCs).

oxidative removal of the 14-α methyl group from lanosterol in the ergosterol biosynthesis pathway. Inhibition of CYP51 is shown to directly deplete ergosterol resulting in the inhibition of fungal growth, making it the primary target for the azole based antifungal drugs.[23] Our results have established that the synthesis of ergosterol is inhibited, which may cause deformation of the cell membrane and its leakage indicating a classical azole based effect on the fungal CYP51. CYP51 is a membrane bound protein that is difficult to purify and structural assessment is only possible by modelling closely related structures. In this study, we have modeled *C. albicans* like CYP51 from *S. cerevisiae*. A structure based sequence alignment showed that CYP51 from *S. cerevisiae* has 65% sequence homology with the CYP51 of *C. albicans* (Fig. 8). The crystal structure of *S. cerevisiae* CYP51 (PDB.4LXJ) was used as a template to

```
                    Identities                Positives
                    339/512 (65%)             411/521(78%)

CP51   4   VETVIDGINYFLSLSVTQQISILLGVPFVYNLVWQYLYSLRKDRAPLVFYWIPWFGSAAS   63
           +E V  G+++FL+L + Q+IS+++ +PF+YN+VWQ LYSLRKDR PLVFYWIPW GSA
4LXJ  12   LEYVNIGLSHFLALPLAQRISLIIIIPFIYNIVWQLLYSLRKDRPPLVFYWIPWVGSAVV   71

CP51  64   YGQQPYEFFESCRQKYGDVFSFMLLGKIMTVYLGPKGHEFVFNAKLSDVSAEDAYKHLTT  123
           YG +PYEFFE C++KYGD+FSF+LLG++MTVYLGPKGHEFVFNAKL+DVSAE AY HLTT
4LXJ  72   YGMKPYEFFEECQKKYGDIFSFVLLGRVMTVYLGPKGHEFVFNAKLADVSAEAAYAHLTT  131

CP51 124   PVFGKGVIYDCPNSRLMEQKKFAKFALTTDSFKRYVPKIREEILNYFVTDESFKLKEKTH  183
           PVFGKGVIYDCPNSRLMEQKKF K ALT ++FK YVP I EE+  YF  ++F+L E+T
4LXJ 132   PVFGKGVIYDCPNSRLMEQKKFVKGALTKEAFKSYVPLIAEEVYKYFRDSKNFRLNERTT  191

CP51 184   GVANVMKTQPEITIFTASRSLFGDEMRRIFDRSFAQLYSDLDKGFTPINFVFPNLPLPHY  243
           G +VM TQPE+TIFTASRSL G EMR  D  FA LYSDLDKGFTPINFVFPNLPL HY
4LXJ 192   GTIDVMVTQPEMTIFTASRSLLGKEMRAKLDTDFAYLYSDLDKGFTPINFVFPNLPLEHY  251

CP51 244   WRRDAAQKKISATYMKEIKSRRERGDIDPNRDLIDSLLIHSTYKDGVKMTDQEIANLLIG  303
           +RD AQK IS TYM  IK RR+  DI  +RDLIDSL+ +STYKDGVKMTDQEIANLLIG
4LXJ 252   RKRDHAQKAISGTYMSLIKERRKNNDIQ-DRDLIDSLMKNSTYKDGVKMTDQEIANLLIG  310

CP51 304   ILMGGQHTSASTSAWFLLHLGEKPHLQDVIYQEVVELLKEKGGDLNDLTYEDLQKLPSVN  363
           +LMGGQHTSA+TSAW LLHL E+P +Q  +Y+E + +L   G  +LTY+ LQ++P +N
4LXJ 311   VLMGGQHTSAATSAWILLHLAERPDVQQELYEEQMRVLD---GGKKELTYDLLQEMPLLN  367

CP51 364   NTIKETLRMHMPLHSIFRKVTNPLRIPETNYIVPKGHYVLVSPGYAHTSERYFDNPEDFD  423
           TIKETLRMH PLHS+FRKV  + +P T+Y++P G++VLVSPGY H  + YF N  F+
4LXJ 368   QTIKETLRMHHPLHSLFRKVMKDMHVPNTSYVIPAGYHVLVSPGYTHLRDEYFPNAHQFN  427

CP51 424   PTRWDTAAAKANSVSFNSSDEVDYGFGKVSKGVSSPYLPFGGGRHRCIGEQFAYVQLGTI  483
           RW+ +A + SV   +EVDYGFG +SKGVSSPYLPFGGGRHRCIGE FAY QLG +
4LXJ 428   IHRWNNDSASSYSV----GEEVDYGFGAISKGVSSPYLPFGGGRHRCIGEHFAYCQLGVL  483

CP51 484   LTTFVYNLRWTI-DGYKVPDPDYSSMVVLPTEPAEIIWEKR  523
           ++ F+  L+W  +G  VP PD++SMV LPT PA+IIWEKR
4LXJ 484   MSIFIRTLKWHYPEGKTVPPPDFTSMVTLPTGPAKIIWEKR  524
```

Fig. 8 Structure based sequence alignment of CYP51 from *S. cerevisiae* and CYP51 of *C. albicans*.

construct a model of *C. albicans* CYP51. The model was further refined using energy minimization and molecular dynamics simulation. We generated 5 model structures for CYP51 from *C. albicans* and checked their Ramachandaran plot values. Among the 5 models, model 3 showed a nearly 89% Ramachandaran value, by careful analysis of the residues in the disallowed region. Structural superimposition of model 3 with its template 4LXJ, showed an RMSD value of 0.248 across 501 atom pairs (Fig. 9A). The mode of binding of lead inhibitors **68** and **70** with modeled *C. albicans* like CYP51 was identified using molecular docking with Autodock Vina and Ligplot (Fig. 9B–E). Since both lead compounds have an azole group flanked by fluorobenzyl and hydrophobic side chains (Phe in **68** and Trp in **70**) we have also performed hydrophobic interaction analysis using LIGPLOT to better characterize the interactions that leads to *in vitro* antifungal activity. The results revealed that proline attached to azole showed significantly less hydrogen bonding and hydrophobic interactions and the compounds were consequently less effective as inhibitors (Tables 1 and 2). Tryptophan and phenylalanine based compounds **68** and **70** with a common terminal *p*-fluorobenzyl group (Table 1) are shown to be more effective inhibitors. The center of the active site is positioned between the I and F helices with heme sitting in the center of the core. Docking studies showed that both **68** and **70** were bound very close to the heme group in the active site pocket of CYP51 interacting with active site residues with high binding affinities (**68** = −10.1 kcal mol^{-1} and **70** = −9.2 kcal mol^{-1}). A longer side chain of the compound compared to the fluconazole appeared to be accommodated in the active site pocket (Fig. 9B and D). The amino group of compound **68** formed a H-bond with the Ser506 residue and the terminal *p*-fluorobenzyl group was very close to the heme, residue Ser506 in the β-turn connecting β4-1 and β4-2 and interacted with the heme group. A number of hydrophobic interactions were observed with Leu376, Phe228, Tyr132, Ile131 and Thr122 (Fig. 9B and C). The terminal *p*-fluorobenzyl group of the inhibitor was found to be extremely close to the Tyr132 and Phe228 phenyl rings showing a possible π–π stacking. Tyr132 has been found to play an important role in fluconazole susceptibility of CYP51 with a fluconazole resistant isolate of *C. albicans* showing mutation in Tyr132.[24] Lead compound **70** similarly showed hydrogen bonding with Asp214 and Glu194 with the side chain of tryptophan at the entrance of the substrate binding pocket. A number of important hydrophobic interactions were detected with Gln309, Ser222, Tyr221, Ala218, Phe213 and Ile197, all these residues are parts of the helix F, helix I and FG loop in the active site pocket of the CYP51 (Fig. 9D and E). Several residues that are important in the active site were identified as common residues that showed interaction with both **68** and **70** and interacted laterally and spanned the length of the active site close to the heme group. The N-terminal of the helix I together with the BC loop forms the entrance of the substrate access channel and a strong interaction close to the substrate binding site might affect the architecture of the active site which can distort the specificity

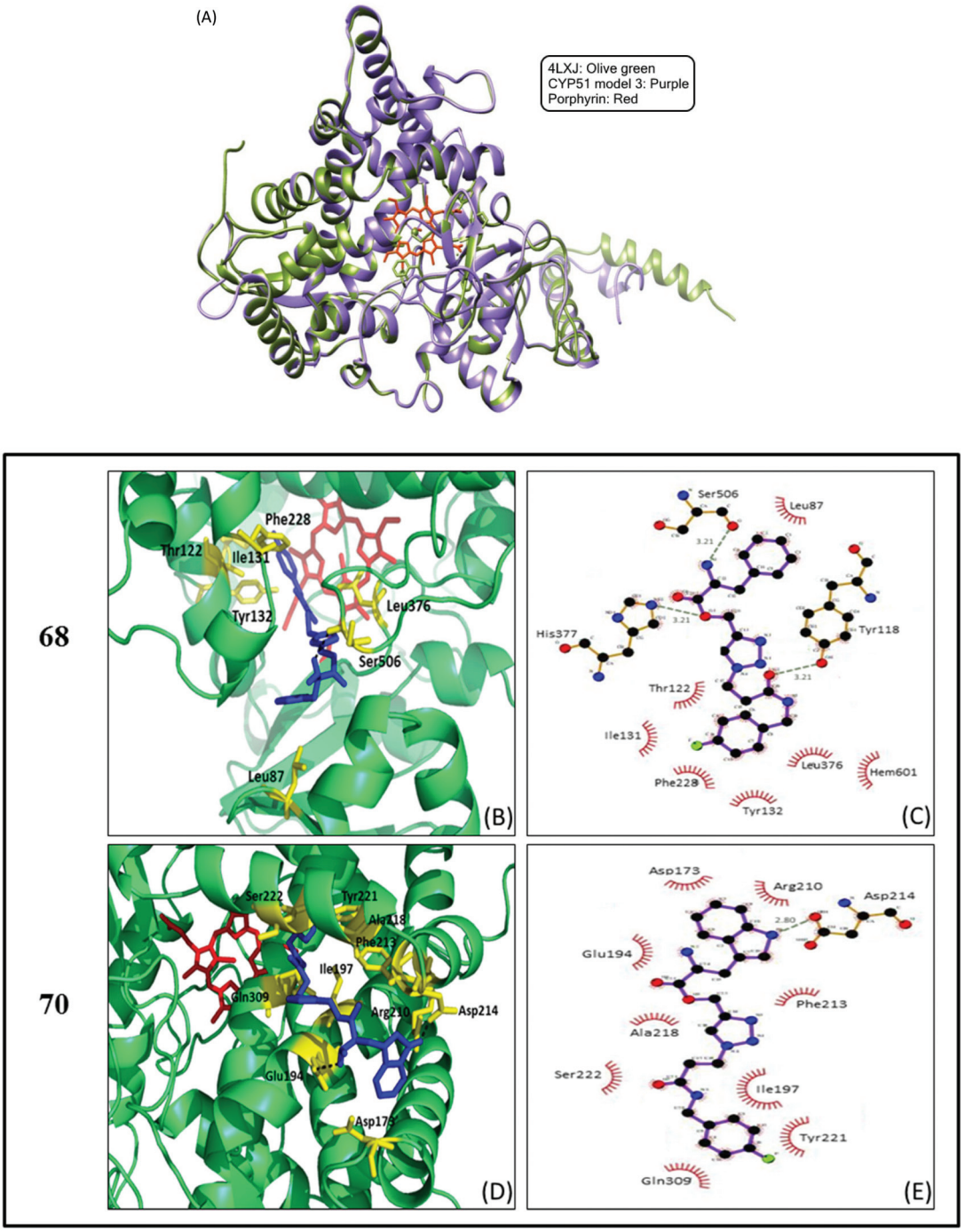

Binding energy: **68** = -10.1 kcal/mol; **70**= -9.2 kcal/mol

Fig. 9 (A) Structural superimposition of model 3 with its template 4LXJ; (B) the plausible mode of binding of **68** in the active site of modeled CYP51; (C) LIGPLOT analysis of binding of **68**; (D) the possible mode of binding of **70** in the active site of modeled CYP51; (E) LIGPLOT analysis of binding of **70**. Binding energy: **68** = –10.1 kcal mol^{-1}; **70** = –9.2 kcal mol^{-1}.

of the substrate. In the absence of the crystal structure of CYP51 from *C. albicans* interacting with its natural substrate, the interaction with the modeled CYP51 provides a rationale for designing lead inhibitors based on the active site and optimization of the structure activity relationship.

In vivo assessment against *Galleria mellonella*

The insect immune response bears many similarities to the innate immune response of mammals and as a consequence insects may be used to evaluate the virulence of microbial

pathogens or assess the toxicity of antimicrobial drugs. The larvae of *G. mellonella* have been used previously to assess the toxicity of novel antifungal compounds and the results showed a strong correlation with those obtained using mammals.[25] An *in vivo* study on the larvae of *G. mellonella* indicated significant anticandidal potential of compounds **68** and **70**. The viability of larvae was not affected following the administration of the compounds up to a concentration of 2.5 mg mL^{-1} which showed a non-toxic behaviour towards the larvae (Fig. 10A–C). Again, at the same concentration no significant alteration in the haemocyte density of the larvae was found which indicated the lack of an immune response (Fig. 10D). The administration of a dose of 2.5 mg mL^{-1} of compounds **68** and **70** to the larvae previously infected with *C. albicans* reduced yeast replication *in vivo* by 50% and 70%, respectively, as measured at 24 h (Fig. 10E).

Experimental section

Chemistry

All the chemicals and solvents (analytical grade) were purchased from Sigma-Aldrich, USA. Thin-layer chromatographic analysis was carried out on precoated Merck silica gel 60 F_{254} TLC aluminium sheets and the spots were visualized under UV light at 254 nm, by iodine-vapor staining or ninhydrin test. IR spectra were recorded on an Agilent Cary 630 FT-IR spectrometer. ^{1}H and ^{13}C NMR spectra were obtained in $CDCl_3$/DMSO-d_6 as a solvent with tetramethylsilane (TMS) as an internal standard on either a Bruker Spectrospin DPX-300 spectrometer at 300 MHz and 75 MHz, respectively, or a Bruker Avance II 400 spectrometer at 400 MHz. 2D spectra (COSY and HETCOR) were recorded on a Jeol, JNM-EXCP 400 spectrometer. Splitting patterns are designated as follows: s (singlet), d (doublet), t (triplet), q (quartet), m (multiplet) or brs (broad). ^{1}H NMR chemical shift (δ) values are reported in parts per million (ppm) relative to the residual solvent ($CDCl_3$, δ 7.26 and DMSO-d_6, δ 2.54). ^{13}C NMR chemical shifts (δ) are reported in ppm relative to $CDCl_3$, δ 77.16 and DMSO-d_6, δ 39.5 and coupling constants (J) are expressed in hertz (Hz). Mass spectra were recorded on a Waters Tandem Quadrupole Detector (TQD) integrated with an electron spray ionization mass spectrometer and on an Agilent RRLC MS 6320 Ion Trap spectrometer fitted with an electrospray ionization (ESI) interface. Melting points were measured on a digital Buchi melting point apparatus (M-560) and are uncorrected. The specific rotation of **41–64** was recorded on an Anton Paar MCP-100 digital polarimeter at 20 °C using sodium D light at a conc. of 1 g per 100 mL in ethanol. Purification of the compounds was carried out by silica gel column chromatography (230–400 mesh size, Merck, Germany) with the indicated eluent.

General procedure for the synthesis of oximes (9–16). Example: synthesis of 4-fluorobenzaldehyde oxime (10)

4-Fluorobenzaldehyde oxime was synthesized by reacting 4-fluorobenzaldehyde (**2**) (12 mmol, 1.29 mL) with

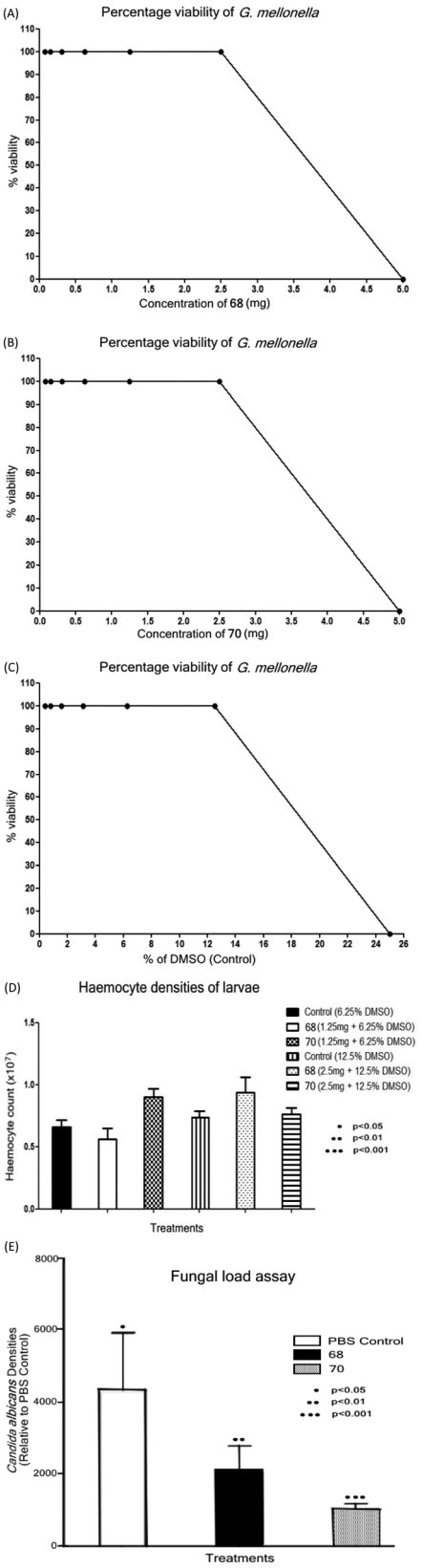

Fig. 10 Percentage viability of *Galleria mellonella* in the presence of (A) **68**; (B) **70**; (C) DMSO; (D) haemocyte densities of larvae and (E) fungal load assay.

hydroxylamine hydrochloride (13 mmol, 0.90 g) in ethanol (20 mL) and pyridine (2.0 mL) mixture under reflux for 21–23 h. After cooling, the solvent was evaporated under *vacuo* and water was added to this residue. This mixture was stirred in an ice bath until the oxime crystallizes. The solid was filtered and washed with water. The product was crystallized from ethanol.[18]

Benzaldehyde oxime (9). Colorless oil, yield 80%. R_f = 0.58 (20% EtOAc in hexane). ^{1}H NMR (300 MHz, $CDCl_3$) δ: 8.67 (s, 1H), 8.17 (s, 1H), 7.59–7.56 (m, 2H), 7.38 (t, J = 3.3 Hz, 3H). IR ν_{max} (neat)/cm^{-1} 3275 (O–H), 1640 (C=N) and 952 (N–O).

4-Fluorobenzaldehyde oxime (10). White solid, yield 84%. R_f = 0.50 (20% EtOAc in hexane). Mp 86–88 °C. ^{1}H NMR (300 MHz, $CDCl_3$) δ: 8.55 (s, 1H), 8.13 (s, 1H), 7.58–7.53 (m, 2H), 7.10–7.05 (m, 2H). IR ν_{max} (neat)/cm^{-1} 3253 (O–H), 1689 (C=N) and 963 (N–O).

4-Chlorobenzaldehyde oxime (11). White solid, yield 89%. R_f = 0.61 (20% EtOAc in hexane). Mp 102–104 °C. ^{1}H NMR (400 MHz, $CDCl_3$) δ: 8.10 (s, 1H), 7.52 (d, J = 8.4 Hz, 2H), 7.36 (d, J = 8.5 Hz, 2H). IR ν_{max} (neat)/cm^{-1} 3257 (O–H), 1659 (C=N) and 959 (N–O).

2-Chlorobenzaldehyde oxime (12). White crystalline solid, yield 94%. R_f = 0.58 (20% EtOAc in hexane). Mp 72–74 °C. ^{1}H NMR (300 MHz, $CDCl_3$) δ: 8.88 (s, 1H), 8.59 (s, 1H), 7.84 (d, J = 7.2 Hz, 1H), 7.41 (d, J = 7.8 Hz, 1H), 7.36–7.26 (m, 2H). IR ν_{max} (neat)/cm^{-1} 3242 (O–H), 1659 (C=N) and 970 (N–O).

4-Methylbenzaldehyde oxime (13). White solid, yield 90%. R_f = 0.56 (20% EtOAc in hexane). Mp 74–76 °C. ^{1}H NMR (400 MHz, $CDCl_3$) δ: 8.10 (s, 1H), 7.52 (d, J = 8.4 Hz, 2H), 7.36 (d, J = 8.4 Hz, 2H), 2.53 (s, 3H). IR ν_{max} (neat)/cm^{-1} 3260 (O–H), 1659 (C=N) and 963 (N–O).

4-Methoxybenzaldehyde oxime (14). Yellow oil, yield 90%. R_f = 0.43 (20% EtOAc in hexane). ^{1}H NMR (400 MHz, $CDCl_3$) δ: 8.10 (s, 1H), 7.52 (d, J = 8.8 Hz, 2H), 6.91 (d, J = 8.8 Hz, 2H), 3.83 (s, 3H). IR ν_{max} (neat)/cm^{-1} 3234 (O–H), 1611 (C=N) and 952 (N–O).

4-(Trifluoromethyl)benzaldehyde oxime (15). Light yellow solid, yield 88%. R_f = 0.55 (20% EtOAc in hexane). Mp 88–90 °C. ^{1}H NMR (400 MHz, $CDCl_3$) δ: 8.17 (s, 1H), 7.70 (d, J = 8.0 Hz, 2H), 7.64 (d, J = 8.4 Hz, 2H). IR ν_{max} (neat)/cm^{-1} 3272 (O–H), 1622 (C=N) and 974 (N–O).

4-(Trifluoromethoxy)benzaldehyde oxime (16). Colourless crystals, yield 90%. R_f = 0.61 (20% EtOAc in hexane). Mp 47–49 °C. ^{1}H NMR (400 MHz, $CDCl_3$) δ: 8.13 (s, 1H), 7.61 (d, J = 8.4 Hz, 2H), 7.24 (d, J = 8.0 Hz, 2H). IR ν_{max} (neat)/cm^{-1} 3267 (O–H), 1696 (C=N) and 977 (N–O).

General procedure for the synthesis of amines (17–24). Example: synthesis of (4-fluorophenyl)methanamine (18)

To a solution of **10** (11.51 mmol, 1.6 g) in ethanol (35 mL), a mixture of water (6.0 mL) and conc. HCl (12 mL) was added. The reaction mixture was stirred at room temperature for 15 min and then it was allowed to cool to 0 °C. Zinc dust (69.04 mmol, 4.38 g) was added slowly to the reaction mixture and it was refluxed for 1 h at 80–90 °C. Progress of the reaction was monitored by TLC. The reaction mixture was filtered and concentrated under *vacuo* to yield the hydrochloride salt of amine. The hydrochloride salt was then treated with dried amberlyst A-21 to afford the corresponding free amine.[18]

Phenylmethanamine (17). Light yellow oil, yield 75%. R_f = 0.0 (40% EtOAc in hexane). ^{1}H NMR (300 MHz, $CDCl_3$) δ: 7.43–7.24 (m, 5H), 3.88 (s, 2H). IR ν_{max} (neat)/cm^{-1} 3367 (NH_2).

(4-Fluorophenyl)methanamine (18). Light yellow oil, yield 82%. R_f = 0.0 (40% EtOAc in hexane). ^{1}H NMR (300 MHz, $CDCl_3$) δ: 7.34–7.26 (m, 2H), 7.06–6.99 (m, 2H), 3.84 (s, 2H). IR ν_{max} (neat)/cm^{-1} 3372 (NH_2).

(4-Chlorophenyl)methanamine (19). Light yellow oil, yield 86%. R_f = 0.0 (40% EtOAc in hexane). ^{1}H NMR (400 MHz, $CDCl_3$) δ: 7.29 (d, J = 8.4 Hz, 2H), 7.24 (d, J = 8.3 Hz, 2H), 3.83 (s, 2H). IR ν_{max} (neat)/cm^{-1} 3365 (NH_2).

(2-Chlorophenyl)methanamine (20). Light yellow oil, yield 78%. R_f = 0.0 (40% EtOAc in hexane). ^{1}H NMR (300 MHz, $CDCl_3$) δ: 7.39–7.36 (m, 2H), 7.28–7.18 (m, 2H), 3.94 (s, 2H). IR ν_{max} (neat)/cm^{-1} 3372 (NH_2).

(4-Methylphenyl)methanamine (21). Light yellow oil, yield 73%. R_f = 0.0 (40% EtOAc in hexane). ^{1}H NMR (400 MHz, $CDCl_3$) δ: 7.20 (d, J = 7.8 Hz, 2H), 7.15 (d, J = 7.9 Hz, 2H), 3.82 (s, 2H), 2.34 (s, 3H). IR ν_{max} (neat)/cm^{-1} 3382 (NH_2).

(4-Methoxyphenyl)methanamine (22). Light yellow oil, yield 81%. R_f = 0.0 (40% EtOAc in hexane). ^{1}H NMR (400 MHz, $CDCl_3$) δ: 7.22 (d, J = 8.5 Hz, 2H), 6.87 (d, J = 8.6 Hz, 2H), 3.79 (brs, 5H). IR ν_{max} (neat)/cm^{-1} 3367 (NH_2).

(4-(Trifluoromethyl)phenyl)methanamine (23). Light yellow oil, yield 67%. R_f = 0.0 (40% EtOAc in hexane). ^{1}H NMR (400 MHz, $CDCl_3$) δ: 7.91 (d, J = 8.0 Hz, 2H), 7.69 (d, J = 7.9 Hz, 2H), 3.95 (s, 2H). IR ν_{max} (neat)/cm^{-1} 3384 (NH_2).

(4-(Trifluoromethoxy)phenyl)methanamine (24). Light yellow oil, yield 71%. R_f = 0.0 (40% EtOAc in hexane). ^{1}H NMR (400 MHz, $CDCl_3$) δ: 7.95 (d, J = 8.6 Hz, 2H), 7.35 (d, J = 8.3 Hz, 2H), 4.52 (s, 2H). IR ν_{max} (neat)/cm^{-1} 3394 (NH_2).

General procedure for the synthesis of azides (27–34). Example: synthesis of *N*-(4-fluorobenzyl)-3-azidopropanamide (28)

To a solution of 3-bromopropionic acid, **25** (19.61 mmol, 3.0 g) in anhyd. DMF (10 mL) was added sodium azide (39.22 mmol, 2.55 g). The reaction mixture was heated at 85 °C for 3 h. The crude reaction mixture was diluted with ethyl acetate which was then washed with 0.1 N HCl, water and brine. The organic layer was dried over anhyd. sodium sulphate, filtered and concentrated under *vacuo* to yield 3-azidopropionic acid, **26** which was used directly in the next reaction without further purification.[26] The prepared azido acid (13.03 mmol, 1.5 g) was dissolved in acetonitrile (15 mL) and stirred at 0 °C. To this cold solution, HOBt (15.54 mmol, 2.09 g) and EDC·HCl (14.02 mmol, 2.69 g) were added. The reaction was stirred for 40 min and then a mixture of NMM (15.54 mmol, 1.71 mL) and **18** (13.03 mmol, 1.28 mL) was added. The reaction mixture was stirred overnight at room temperature. The solid was filtered and the acetonitrile was removed under *vacuo*. The residue was dissolved in 50 mL ethyl acetate, washed with

saturated citric acid solution, 5% aq. sodium bicarbonate solution and brine. The organic layer was dried over anhyd. sodium sulphate, filtered, evaporated and gave crude azide. The crude product was purified by column chromatography eluted by using a solution of ethyl acetate : hexane (4 : 6) to yield pure azide (**28**).[27]

***N*-Benzyl-3-azidopropanamide (27).** Yellow oil, yield 37%. R_f = 0.48 (40% EtOAc in hexane). ^{1}H NMR (300 MHz, $CDCl_3$) δ: 7.38–7.27 (m, 5H), 6.17 (brs, 1H), 4.45 (d, J = 5.7 Hz, 2H), 3.63 (t, J = 6.3 Hz, 2H), 2.45 (t, J = 6.4 Hz, 2H). ^{13}C NMR (75 MHz, $CDCl_3$) δ: 171.45, 141.63, 128.94, 128.66, 127.32, 45.76, 41.56, 33.82. IR ν_{max} (neat)/cm^{-1} 2093 (azide), 1644 (C═O) and 1544 (NH). MS (ESI), m/z: 205.07 $[M + H]^+$.

***N*-(4-Fluorobenzyl)-3-azidopropanamide (28).** Light yellow solid, yield 49%. R_f = 0.45 (40% EtOAc in hexane). Mp 36–38 °C. ^{1}H NMR (300 MHz, $CDCl_3$) δ: 7.28–7.23 (m, 2H), 7.05–6.99 (m, 2H), 6.10 (brs, 1H), 4.42 (d, J = 5.7 Hz, 2H), 3.64 (t, J = 6.3 Hz, 2H), 2.45 (t, J = 6.3 Hz, 2H). ^{13}C NMR (75 MHz, $CDCl_3$) δ: 169.85, 160.58, 133.80, 129.50, 115.73, 47.39, 42.99, 35.82. IR ν_{max} (neat)/cm^{-1} 2086 (azide), 1641 (C═O) and 1553 (NH). MS (ESI), m/z: 223.1 $[M + H]^+$.

***N*-(4-Chlorobenzyl)-3-azidopropanamide (29).** Light yellow solid, yield 36%. R_f = 0.31 (40% EtOAc in hexane). Mp 33–35 °C. ^{1}H NMR (300 MHz, $CDCl_3$) δ: 7.32 (d, J = 8.1 Hz, 2H), 7.23 (d, J = 7.2 Hz, 2H), 6.04 (s, 1H), 4.44 (d, J = 5.4 Hz, 2H), 3.66 (t, J = 6.0 Hz, 2H), 2.47 (t, J = 6.1 Hz, 2H). ^{13}C NMR (75 MHz, $CDCl_3$) δ: 169.98, 136.56, 133.35, 129.04, 128.84, 47.39, 42.96, 35.77. IR ν_{max} (neat)/cm^{-1} 2095 (azide), 1640 (C═O) and 1544 (NH). MS (ESI), *mz*: 239.1 $[M + H]^+$.

***N*-(2-Chlorobenzyl)-3-azidopropanamide (30).** Light yellow solid, yield 39%. R_f = 0.48 (40% EtOAc in hexane). Mp 38–40 °C. ^{1}H NMR (300 MHz, $CDCl_3$) δ: 7.39–7.35 (m, 2H), 7.29–7.22 (m, 2H), 6.26 (brs, 1H), 4.55 (d, J = 5.7 Hz, 2H), 3.63 (t, J = 6.4 Hz, 2H), 2.46 (t, J = 6.3 Hz, 2H). ^{13}C NMR (75 MHz, $CDCl_3$) δ: 169.81, 135.33, 133.63, 130.24, 129.57, 129.08, 127.17, 47.37, 41.65, 35.78. IR ν_{max} (neat)/cm^{-1} 2102 (azide), 1644 (C═O) and 1551 (NH). MS (ESI), m/z: 239.1 $[M + H]^+$.

***N*-(4-Methylbenzyl)-3-azidopropanamide (31).** Yellow oil, yield 53%. R_f = 0.33 (40% EtOAc in hexane). ^{1}H NMR (400 MHz, $CDCl_3$) δ: 7.19–7.14 (m, 4H), 5.80 (brs, 1H), 4.42 (d, J = 5.6 Hz, 2H), 3.66 (t, J = 6.4 Hz, 2H), 2.44 (t, J = 6.4 Hz, 2H), 2.34 (s, 3H). ^{13}C NMR (75 MHz, $CDCl_3$) δ: 169.58, 137.39, 134.88, 129.44, 127.84, 47.44, 43.56, 35.90, 21.08. IR ν_{max} (neat)/cm^{-1} 2102 (azide), 1618 (C═O) and 1585 (NH). MS (ESI), m/z: 218.9 $[M + H]^+$.

***N*-(4-Methoxybenzyl)-3-azidopropanamide (32).** Light yellow solid, yield 41%. R_f = 0.41 (40% EtOAc in hexane). Mp 58–60 °C. ^{1}H NMR (300 MHz, $CDCl_3$) δ: 7.14 (d, J = 8.4 Hz, 2H), 6.80 (d, J = 8.7 Hz, 2H), 5.77 (brs, 1H), 4.32 (d, J = 5.4 Hz, 2H), 3.73 (s, 3H), 3.58 (t, J = 6.4 Hz, 2H), 2.36 (t, J = 6.4 Hz, 2H). ^{13}C NMR (75 MHz, $CDCl_3$) δ: 169.85, 160.58, 133.80, 129.50, 115.73, 57.04, 47.39, 42.99, 35.82. IR ν_{max} (neat)/cm^{-1} 2091 (azide), 1637 (C═O) and 1559 (NH). MS (ESI), m/z: 234.9 $[M + H]^+$.

***N*-(4-(Trifluoromethyl)benzyl)-3-azidopropanamide (33).** Light yellow oil, yield 56%. R_f = 0.43 (40% EtOAc in hexane). ^{1}H NMR (400 MHz, $CDCl_3$) δ: 7.60 (d, J = 8.0 Hz, 2H), 7.40 (d, J = 7.7 Hz, 2H), 5.96 (brs, 1H), 4.53 (d, J = 5.8 Hz, 2H), 3.68 (t, J = 6.2 Hz, 2H), 2.48 (t, J = 6.2 Hz, 2H). ^{13}C NMR (75 MHz, $CDCl_3$) δ: 170.01, 142.05, 129.67, 127.87, 125.71, 122.24, 47.38, 43.18, 35.86. IR ν_{max} (neat)/cm^{-1} 2107 (azide), 1654 (C═O) and 1547 (NH). MS (ESI), m/z: 272.9 $[M + H]^+$, 271.1 $[M - H]^-$.

***N*-(4-(Trifluoromethoxy)benzyl)-3-azidopropanamide (34).** Yellow oil, yield 45%. R_f = 0.27 (40% EtOAc in hexane). ^{1}H NMR (400 MHz, $CDCl_3$) δ: 7.32 (d, J = 8.4 Hz, 2H), 7.19 (d, J = 8.2 Hz, 2H), 5.90 (brs, 1H), 4.46 (d, J = 7.1 Hz, 2H), 3.67 (t, J = 6.2 Hz, 2H), 2.46 (t, J = 6.3 Hz, 2H). ^{13}C NMR (75 MHz, $CDCl_3$) δ: 169.85, 158.72, 134.58, 129.50, 123.53, 115.76, 47.39, 42.99, 35.82. IR ν_{max} (neat)/cm^{-1} 2102 (azide), 1652 (C═O) and 1547 (NH). MS (ESI), m/z: 289.45 $[M + H]^+$.

General procedure for the synthesis of propargyl ester of boc-protected alkynes (38–40). Example: synthesis of propargyl ester of boc-L-phenylalanine (38)

Boc-protected L-phenylalanine (11.31 mmol, 3.0 g) was dissolved in anhyd. DMF (10 mL) and the solution was allowed to cool to 0 °C. Anhyd. potassium carbonate (16.96 mmol, 2.34 g) was added to this cold solution and stirred for 15 min. Propargyl bromide (11.31 mmol, 1.26 mL, 80 wt% in toluene) was added dropwise to the mixture and stirred at 0 °C for 1 h. The reaction mixture was allowed to attain room temperature. After removal of DMF under *vacuo*, the residue was dissolved in ethyl acetate. The organic layer was washed with saturated citric acid solution, water and brine which was dried over anhyd. sodium sulphate and concentrated. The crude product was then purified by column chromatography eluted by using ethyl acetate : hexane (2 : 8) to yield pure alkyne (**38**).[28]

Propargyl ester of boc-L-phenylalanine (38). Light yellow oil, yield 87%. R_f = 0.52 (20% EtOAc in hexane). ^{1}H NMR (300 MHz, $CDCl_3$) δ: 7.34–7.26 (m, 3H), 7.19–7.17 (m, 2H), 4.97 (d, J = 7.5 Hz, 1H), 4.82–4.64 (m, 3H), 3.20–3.06 (m, 2H), 2.53 (s, 1H), 1.43 (s, 9H). ^{13}C NMR (75 MHz, $CDCl_3$) δ: 171.16, 155.07, 135.70, 129.41, 128.61, 127.13, 80.06, 75.47, 54.31, 52.65, 38.10, 28.28. IR ν_{max} (neat)/cm^{-1} 3365 (≡CH), 2129 (C≡C), 1762 (C═O, ester), 1687 (C═O, amide) and 1510 (NH). MS (ESI), m/z: 326.2 $[M + Na]^+$, 629.4 $[2M + Na]^+$.

Propargyl ester of boc-L-proline (39). Light yellow oil, yield 85%. R_f = 0.64 (20% EtOAc in hexane). ^{1}H NMR (300 MHz, $CDCl_3$) δ: 4.78–4.69 (m, 2H), 4.29–4.25 (m, 1H), 3.58–3.40 (m, 2H), 2.48 (s, 1H), 2.26–2.23 (m, 1H), 2.05–1.91 (m, 3H), 1.42 (s, 9H). ^{13}C NMR (75 MHz, $CDCl_3$) δ: 172.42, 153.70, 80.06, 75.11, 58.91, 52.23, 46.30, 30.79, 28.28, 23.61. IR ν_{max} (neat)/cm^{-1} 3246 (≡CH), 2129 (C≡C), 1754 (C═O, ester) and 1693 (C═O, amide). MS (ESI), m/z: 254.4 $[M + H]^+$.

Propargyl ester of boc-L-tryptophan (40). Light yellow solid, yield 88%. R_f = 0.31 (20% EtOAc in hexane). Mp 95–96 °C. ^{1}H NMR (300 MHz, $CDCl_3$) δ: 8.17 (s, 1H), 7.60 (d, J = 7.8 Hz, 1H), 7.38 (d, J = 7.8 Hz, 1H), 7.21–7.12 (m, 2H), 7.07 (s, 1H), 5.08 (d, J = 8.1 Hz, 1H), 4.77–4.63 (m, 3H), 3.35–3.33 (m, 2H), 2.50 (s, 1H), 1.44 (s, 9H). ^{13}C NMR (75 MHz, $CDCl_3$) δ: 171.54, 155.24, 136.12, 127.71, 122.95, 122.24, 119.69, 118.76, 111.20, 109.92, 79.99, 75.37, 54.23, 52.65, 28.32, 27.76. IR ν_{max} (neat)/cm^{-1}

3397 (≡CH), 2147 (C≡C), 1736 (C═O, ester), 1698 (C═O, amide) and 1503 (NH). MS (ESI), *m*/*z*: 365.09 $[M + Na]^+$, 707.4 $[2M + Na]^+$.

Synthesis of boc-protected triazole–amino acid hybrids (41–64). Example: synthesis of (*R*)-(1-(3-(4-fluorobenzylamino)-3-oxopropyl)-1*H*-1,2,3-triazol-4-yl)methyl 2-[(*tert*-butoxycarbonyl)amino]-3-phenylpropanoate (44)

Azide **28** (1.35 mmol, 0.3 g) and alkyne **38** (1.35 mmol, 0.41 g) were dissolved in *tert*-butanol (4.0 mL) and H_2O (8.0 mL). The copper sulphate, $CuSO_4{\cdot}5H_2O$ (0.013 mmol, 0.033 g) and sodium ascorbate (0.067 mmol, 0.013 g) were added and the reaction mixture was stirred at room temperature. Progress of the reaction was monitored by TLC. After completion of the reaction, the content of the reaction was washed with brine and the compound was extracted with ethyl acetate, dried over anhyd. sodium sulphate and concentrated. The product was purified by column chromatography eluted with ethyl acetate : hexane (3 : 7) to yield the pure product in quantitative yield.[29]

(*R*)-(1-(3-(Benzylamino)-3-oxopropyl)-1*H*-1,2,3-triazol-4-yl)methyl 2-[(*tert*-butoxycarbonyl)amino]-3-phenylpropanoate (41). Off white solid, yield 86%. R_f = 0.76 (10% MeOH in DCM). Mp 93–95 °C. $[\alpha]_D^{20}$ = −28.00. ^{1}H NMR (300 MHz, $CDCl_3$) δ: 7.50 (s, 1H), 7.26–7.15 (m, 7H), 7.10 (d, *J* = 7.5 Hz, 2H), 6.99–6.97 (m, 1H), 5.91 (brs, 1H), 5.14 (s, 2H), 4.88 (d, *J* = 7.2 Hz, 1H), 4.62 (t, *J* = 5.6 Hz, 2H), 4.47–4.45 (m, 1H), 4.32 (d, *J* = 5.7 Hz, 2H), 3.02–2.95 (m, 2H), 2.78 (t, *J* = 6.3 Hz, 2H), 1.33 (s, 9H). ^{13}C NMR (75 MHz, $CDCl_3$) δ: 171.65, 168.99, 155.08, 142.07, 137.79, 135.82, 129.33, 128.69, 128.50, 127.69, 127.59, 126.99, 125.09, 80.03, 58.23, 54.40, 46.25, 43.67, 38.05, 36.32, 28.28. IR ν_{max} (neat)/cm^{-1} 3078 (CH), 1598 (C═C) and 1460 (N═N). MS (ESI), *m*/*z*: 508.3 $[M + H]^+$.

(*R*)-(1-(3-(Benzylamino)-3-oxopropyl)-1*H*-1,2,3-triazol-4-yl) methyl 1-(*tert*-butoxycarbonyl)pyrrolidine-2-carboxylate (42). Light yellow oil, yield 84%. R_f = 0.84 (10% MeOH in DCM). $[\alpha]_D^{20}$ = −48.00. ^{1}H NMR (300 MHz, $CDCl_3$) δ: 7.71 (s, 1H), 7.31–7.19 (m, 5H), 6.04 (brs, 1H), 5.26–5.21 (m, 2H), 4.73–4.71 (m, 2H), 4.41 (s, 2H), 4.25–4.16 (m, 1H), 3.53–3.39 (m, 2H), 2.89–2.84 (m, 2H), 2.21–2.15 (m, 1H), 1.94–1.86 (m, 3H), 1.45 (s, 9H). ^{13}C NMR (75 MHz, $CDCl_3$) δ: 173.02, 168.97, 154.44, 142.91, 137.75, 128.70, 127.69, 124.98, 79.94, 58.99, 57.94, 46.63, 43.66, 36.58, 30.79, 29.79, 28.41, 24.33. IR ν_{max} (neat)/cm^{-1} 3067 (CH), 1549 (C═C) and 1454 (N═N). MS (ESI), *m*/*z*: 358.3 $[M + H - Boc]^+$, 458.4 $[M + H]^+$.

(*R*)-(1-(3-(Benzylamino)-3-oxopropyl)-1*H*-1,2,3-triazol-4-yl)methyl 2-[(*tert*-butoxycarbonyl)amino]-3-(1*H*-indol-3-yl)propanoate (43). Light yellow solid, yield 92%. R_f = 0.67 (10% MeOH in DCM). Mp 68–70 °C. $[\alpha]_D^{20}$ = −20.00. ^{1}H NMR (300 MHz, $CDCl_3$) δ: 8.74 (s, 1H), 7.47 (d, *J* = 7.8 Hz, 1H), 7.30 (d, *J* = 7.8 Hz, 1H), 7.26–7.19 (m, 4H), 7.12–6.99 (m, 4H), 6.46 (s, 1H), 6.13 (s, 1H), 5.23–5.16 (m, 1H), 5.04–5.00 (m, 2H), 4.60–4.44 (m, 3H), 4.32 (t, *J* = 6.0 Hz, 2H), 3.16–3.14 (m, 2H), 2.90–2.77 (m, 2H), 1.37 (s, 9H). ^{13}C NMR (75 MHz, $CDCl_3$) δ: 172.12, 169.48, 155.24, 142.43, 137.63, 136.09, 128.74, 127.61, 127.51, 124.99, 123.29, 121.91, 119.45, 118.75, 111.34, 109.41, 79.97, 58.23, 54.52, 46.11, 43.71, 35.64, 28.35, 28.06. IR ν_{max} (neat)/cm^{-1} 3060 (CH), 1525 (C═C) and 1458 (N═N). MS (ESI), *m*/*z*: 547.3 $[M + H]^+$.

(*R*)-(1-(3-(4-Fluorobenzylamino)-3-oxopropyl)-1*H*-1,2,3-triazol-4-yl)methyl 2-[(*tert*-butoxycarbonyl)amino]-3-phenylpropanoate (44). Creamish solid, yield 89%. R_f = 0.77 (10% MeOH in DCM). Mp 88–90 °C. $[\alpha]_D^{20}$ = −4.00. ^{1}H NMR (300 MHz, $CDCl_3$) δ: 7.57 (s, 1H), 7.22 (m, 3H), 7.14 (brs, 2H), 7.06 (brs, 2H), 7.00–6.95 (m, 2H), 6.36 (brs, 1H), 5.19 (s, 2H), 4.96 (brs, 1H), 4.67 (brs, 2H), 4.51 (m, 1H), 4.35 (brs, 2H), 3.04 (m, 2H), 2.86 (brs, 2H), 1.39 (s, 9H). ^{13}C NMR (75 MHz, $CDCl_3$) δ: 171.66, 168.97, 160.77, 155.33, 142.18, 140.27, 135.81, 133.66, 129.47, 128.52, 127.01, 125.03, 115.39, 80.07, 58.23, 54.44, 46.23, 42.96, 38.05, 36.30, 28.27. IR ν_{max} (neat)/cm^{-1} 3057 (CH), 1514 (C═C) and 1458 (N═N). MS (ESI), *m*/*z*: 526.1 $[M + H]^+$, 548.1 $[M + Na]^+$.

(*R*)-(1-(3-(4-Fluorobenzylamino)-3-oxopropyl)-1*H*-1,2,3-triazol-4-yl)methyl 1-(*tert*-butoxycarbonyl)pyrrolidine-2-carboxylate (45). Light yellow oil, yield 80%. R_f = 0.70 (10% MeOH in DCM). $[\alpha]_D^{20}$ = −44.00. ^{1}H NMR (300 MHz, $CDCl_3$) δ: 7.73 (d, *J* = 11.1 Hz, 1H), 7.20–7.12 (m, 2H), 7.04–6.97 (m, 2H), 6.55 (brs, 1H), 5.33–5.22 (m, 2H), 4.79–4.66 (m, 2H), 4.39–4.37 (m, 2H), 4.26–4.23 (m, 1H), 3.52–3.39 (m, 2H), 2.92–2.85 (m, 2H), 2.21–1.84 (m, 4H), 1.44 (s, 9H). ^{13}C NMR (75 MHz, $CDCl_3$) δ: 172.99, 169.24, 153.67, 142.68, 138.75, 134.33, 129.39, 124.95, 115.37, 79.83, 58.92, 46.63, 46.28, 42.59, 35.96, 30.76, 28.39, 23.59. IR ν_{max} (neat)/cm^{-1} 3075 (CH), 1512 (C═C) and 1452 (N═N). MS (ESI), *m*/*z*: 376.05 $[M + H - Boc]^+$, 476.04 $[M + H]^+$, 498.2 $[M + Na]^+$.

(*R*)-(1-(3-(4-Fluorobenzylamino)-3-oxopropyl)-1*H*-1,2,3-triazol-4-yl)methyl 2-[(*tert*-butoxycarbonyl)amino]-3-(1*H*-indol-3-yl)propanoate (46). Light yellow solid, yield 90%. R_f = 0.71 (10% MeOH in DCM). Mp 62–64 °C. $[\alpha]_D^{20}$ = −20.00. ^{1}H NMR (300 MHz, $CDCl_3$) δ: 8.88 (s, 1H, NH), 7.53 (d, *J* = 7.5 Hz, 1H, Ar–H), 7.35 (d, *J* = 8.1 Hz, 1H, Ar–H), 7.17–7.05 (m, 5H, Ar–H), 6.96 (t, *J* = 8.6 Hz, 2H, Ar–H), 6.56–6.52 (m, 2H, Ar–H, NH), 5.25–5.21 (m, 1H, NH), 5.14–5.05 (m, 2H, OCH_2), 4.65–4.49 (m, 3H, CH, CH_2), 4.33–4.32 (m, 2H, CH_2), 3.23 (brs, 2H, CH_2), 2.94–2.82 (m, 2H, CH_2), 1.43 (s, 9H, Boc). ^{13}C NMR (75 MHz, $CDCl_3$) δ: 172.11, 169.45, 163.82, 155.26, 142.52, 136.09, 133.43, 129.31, 127.74, 125.01, 123.22, 121.97, 119.49, 118.76, 115.69, 111.29, 109.48, 79.98, 58.21, 54.51, 46.08, 43.01, 35.59, 28.33, 27.97. IR ν_{max} (neat)/cm^{-1} 3080 (CH), 1512 (C═C) and 1460 (N═N). MS (ESI), *m*/*z*: 565.3 $[M + H]^+$.

(*R*)-(1-(3-(4-Chlorobenzylamino)-3-oxopropyl)-1*H*-1,2,3-triazol-4-yl)methyl 2-[(*tert*-butoxycarbonyl)amino]-3-phenylpropanoate (47). White solid, yield 88%. R_f = 0.72 (10% MeOH in DCM). Mp 98–100 °C. $[\alpha]_D^{20}$ = −16.00. ^{1}H NMR (300 MHz, $CDCl_3$) δ: 7.56 (s, 1H), 7.27–7.22 (m, 5H), 7.10–7.04 (m, 4H), 6.60 (brs, 1H), 5.18 (s, 2H), 4.98 (d, *J* = 7.8 Hz, 1H), 4.68–4.63 (m, 2H), 4.50–4.46 (m, 1H), 4.34 (d, *J* = 5.7 Hz, 2H), 3.08–2.98 (m, 2H), 2.87 (t, *J* = 6.3 Hz, 2H), 1.39 (s, 9H). ^{13}C NMR (75 MHz, $CDCl_3$) δ: 171.66, 169.09, 155.13, 142.17, 136.45, 135.79, 133.32, 129.31, 129.04, 128.78, 128.52, 127.02, 125.07, 80.06, 58.20, 54.43, 46.25, 42.93, 38.01, 36.26, 28.27. IR ν_{max} (neat)/cm^{-1} 3067 (CH), 1521 (C═C) and 1462 (N═N). MS (ESI), *m*/*z*: 542.5 $[M + H]^+$.

(*R*)-(1-(3-(4-Chlorobenzylamino)-3-oxopropyl)-1*H*-1,2,3-triazol-4-yl)methyl 1-(*tert*-butoxycarbonyl)pyrrolidine-2-carboxylate (48). Colorless oil, yield 87%. R_f = 0.67 (10% MeOH in DCM). $[\alpha]_D^{20}$ = −44.00. ^{1}H NMR (300 MHz, $CDCl_3$) δ: 7.62 (s, 1H), 7.19 (d, J = 9.0 Hz, 2H), 7.05–6.98 (m, 2H), 6.59 (brs, 1H), 5.17–5.10 (m, 2H), 4.68–4.51 (m, 2H), 4.29–4.24 (m, 2H), 4.20–4.16 (m, 1H), 3.41–3.27 (m, 2H), 2.84–2.74 (m, 2H), 2.11–1.98 (m, 2H), 1.86–1.77 (m, 2H), 1.35–1.26 (m, 9H). ^{13}C NMR (75 MHz, $CDCl_3$) δ: 173.02, 169.15, 154.46, 143.01, 136.57, 133.31, 129.05, 128.76, 125.02, 79.97, 58.99, 58.06, 46.67, 42.89, 36.59, 30.78, 29.78, 28.41, 24.34. IR ν_{max} (neat)/cm^{-1} 3089 (CH), 1547 (C═C) and 1495 (N═N). MS (ESI), m/z: 392.5 $[M + H - Boc]^+$, 492.4 $[M + H]^+$.

(*R*)-(1-(3-(4-Chlorobenzylamino)-3-oxopropyl)-1*H*-1,2,3-triazol-4-yl)methyl 2-[(*tert*-butoxycarbonyl)amino]-3-(1*H*-indol-3-yl)propanoate (49). Light yellow solid, yield 87%. R_f = 0.73 (10% MeOH in DCM). Mp 70–72 °C. $[\alpha]_D^{20}$ = −20.00. ^{1}H NMR (300 MHz, $CDCl_3$) δ: 8.88 (s, 1H), 7.53 (d, J = 7.5 Hz, 1H), 7.34 (d, J = 8.1 Hz, 1H), 7.26–7.22 (m, 2H), 7.18–7.13 (m, 2H), 7.10–7.03 (m, 3H), 6.65 (brs, 1H), 6.53 (s, 1H), 5.25–5.20 (m, 1H), 5.09–5.04 (m, 2H), 4.64–4.48 (m, 3H), 4.31 (d, J = 6.0 Hz, 2H), 3.23–3.21 (m, 2H), 2.94–2.82 (m, 2H), 1.43 (s, 9H). ^{13}C NMR (75 MHz, $CDCl_3$) δ: 172.12, 169.56, 155.26, 142.51, 136.26, 136.08, 133.33, 128.86, 128.80, 127.72, 125.04, 123.24, 121.96, 119.49, 118.75, 111.31, 109.45, 79.99, 58.19, 54.50, 46.10, 42.99, 35.55, 28.33, 27.97. IR ν_{max} (neat)/cm^{-1} 3083 (CH), 1514 (C═C) and 1462 (N═N). MS (ESI), m/z: 579.2 $[M - H]^-$, 581.1 $[M + H]^+$.

(*R*)-(1-(3-(2-Chlorobenzylamino)-3-oxopropyl)-1*H*-1,2,3-triazol-4-yl)methyl 2-[(*tert*-butoxycarbonyl)amino]-3-phenylpropanoate (50). White solid, yield 84%. R_f = 0.73 (10% MeOH in DCM). Mp 118–120 °C. $[\alpha]_D^{20}$ = −16.00. ^{1}H NMR (300 MHz, $CDCl_3$) δ: 7.48 (s, 1H), 7.29–7.13 (m, 7H), 6.99–6.97 (m, 2H), 6.05 (brs, 1H), 5.13 (s, 2H), 4.89 (d, J = 7.5 Hz, 1H), 4.61 (t, J = 5.8 Hz, 2H), 4.48–4.47 (m, 1H), 4.41 (d, J = 5.7 Hz, 2H), 3.05–2.90 (m, 2H), 2.78 (t, J = 6.2 Hz, 2H), 1.33 (s, 9H). ^{13}C NMR (75 MHz, $CDCl_3$) δ: 171.60, 168.97, 155.28, 143.42, 137.44, 135.82, 133.62, 130.05, 129.52, 129.29, 129.07, 128.45, 127.05, 126.94, 125.33, 79.98, 58.20, 54.31, 46.10, 41.60, 37.98, 36.24, 28.23. IR ν_{max} (neat)/cm^{-1} 3062 (CH), 1521 (C═C) and 1445 (N═N). MS (ESI), m/z: 542.1 $[M + H]^+$.

(*R*)-(1-(3-(2-Chlorobenzylamino)-3-oxopropyl)-1*H*-1,2,3-triazol-4-yl)methyl 1-(*tert*-butoxycarbonyl)pyrrolidine-2-carboxylate (51). Colorless oil, yield 83%. R_f = 0.77 (10% MeOH in DCM). $[\alpha]_D^{20}$ = −48.00. ^{1}H NMR (300 MHz, $CDCl_3$) δ: 7.69 (d, J = 7.5 Hz, 1H), 7.39–7.23 (m, 4H), 6.43 (brs, 1H), 5.26–5.20 (m, 2H), 4.78–4.63 (m, 2H), 4.50 (d, J = 5.4 Hz, 2H), 4.26–4.23 (m, 1H), 3.55–3.39 (m, 2H), 2.91–2.83 (m, 2H), 2.21–2.10 (m, 1H), 1.95–1.84 (m, 3H), 1.45 (s, 9H). ^{13}C NMR (75 MHz, $CDCl_3$) δ: 173.21, 167.98, 154.44, 142.91, 137.75, 133.45, 128.70, 126.98, 124.98, 79.94, 58.10, 57.99, 46.44, 43.66, 36.58, 30.79, 29.79, 28.41, 23.60. IR ν_{max} (neat)/cm^{-1} 3073 (CH), 1544 (C═C) and 1447 (N═N). MS (ESI), m/z: 492.3 $[M + H]^+$.

(*R*)-(1-(3-(2-Chlorobenzylamino)-3-oxopropyl)-1*H*-1,2,3-triazol-4-yl)methyl 2-[(*tert*-butoxycarbonyl)amino]-3-(1*H*-indol-3-yl)propanoate (52). Light yellow solid, yield 88%. R_f = 0.41 (10% MeOH in DCM). Mp 58–62 °C. $[\alpha]_D^{20}$ = −16.00. ^{1}H NMR (300 MHz, $CDCl_3$) δ: 8.83 (s, 1H), 7.56 (d, J = 7.8 Hz, 1H), 7.41–7.35 (m, 3H), 7.29–7.08 (m, 5H), 6.60 (s, 1H), 6.36 (brs, 1H), 5.29–5.25 (m, 1H), 5.14–5.09 (m, 2H), 4.68–4.54 (m, 3H), 4.49 (brs, 2H), 3.26–3.19 (m, 2H), 2.95–2.88 (m, 2H), 1.46 (s, 9H). ^{13}C NMR (75 MHz, $CDCl_3$) δ: 172.12, 169.54, 155.24, 142.43, 136.07, 134.96, 133.48, 129.73, 129.59, 129.09, 127.75, 127.11, 125.02, 123.28, 121.92, 119.46, 118.78, 111.32, 109.42, 79.96, 58.24, 54.48, 46.02, 41.70, 35.53, 28.35, 28.02. IR ν_{max} (neat)/cm^{-1} 3067 (CH), 1514 (C═C) and 1447 (N═N). MS (ESI), m/z: 581.3 $[M + H]^+$.

(*R*)-(1-(3-(4-Methylbenzylamino)-3-oxopropyl)-1*H*-1,2,3-triazol-4-yl)methyl 2-[(*tert*-butoxycarbonyl)amino]-3-phenylpropanoate (53). Creamish solid, yield 90%. R_f = 0.63 (10% MeOH in DCM). Mp 105–107 °C. $[\alpha]_D^{20}$ = −16.00. ^{1}H NMR (300 MHz, $CDCl_3$) δ: 7.57 (s, 1H), 7.26–7.21 (m, 3H), 7.11–7.04 (m, 6H), 6.34 (brs, 1H), 5.21 (s, 2H), 4.99 (d, J = 7.8 Hz, 1H), 4.65 (t, J = 6.3 Hz, 2H), 4.56–4.50 (m, 1H), 4.33 (d, J = 5.7 Hz, 2H), 3.11–2.96 (m, 2H), 2.83 (t, J = 6.3 Hz, 2H), 2.31 (s, 3H), 1.40 (s, 9H). ^{13}C NMR (75 MHz, $CDCl_3$) δ: 171.64, 168.88, 155.09, 142.05, 137.32, 135.83, 134.74, 129.36, 128.49, 127.72, 126.99, 125.08, 80.02, 58.24, 54.40, 46.23, 43.45, 38.05, 36.35, 28.27, 21.07. IR ν_{max} (neat)/cm^{-1} 3067 (CH), 1521 (C═C) and 1462 (N═N). MS (ESI), m/z: 522.2 $[M + H]^+$.

(*R*)-(1-(3-(4-Methylbenzylamino)-3-oxopropyl)-1*H*-1,2,3-triazol-4-yl)methyl 1-(*tert*-butoxycarbonyl)pyrrolidine-2-carboxylate (54). Colorless oil, yield 83%. R_f = 0.67 (10% MeOH in DCM). $[\alpha]_D^{20}$ = −48.00. ^{1}H NMR (300 MHz, $CDCl_3$) δ: 7.70 (s, 1H), 7.12–7.03 (m, 4H), 6.45 (brs, 1H), 5.19 (m, 2H), 4.69–4.64 (m, 2H), 4.34–4.32 (m, 2H), 4.23–4.19 (m, 1H), 3.51–3.37 (m, 2H), 2.87–2.79 (m, 2H), 2.31 (s, 3H), 2.19–2.12 (m, 2H), 1.95–1.81 (m, 3H), 1.42 (s, 9H). ^{13}C NMR (75 MHz, $CDCl_3$) δ: 172.99, 168.94, 154.42, 142.83, 137.26, 134.86, 129.32, 127.70, 124.97, 79.92, 58.98, 58.08, 46.62, 43.38, 36.52, 30.78, 29.78, 28.40, 24.33, 21.05. IR ν_{max} (neat)/cm^{-1} 3089 (CH), 1547 (C═C) and 1454 (N═N). MS (ESI), m/z: 358.3 $[M + H - Boc]^+$, 471.99 $[M + H]^+$, 494.13 $[M + Na]^+$.

(*R*)-(1-(3-(4-Methylbenzylamino)-3-oxopropyl)-1*H*-1,2,3-triazol-4-yl)methyl 2-[(*tert*-butoxycarbonyl)amino]-3-(1*H*-indol-3-yl)propanoate (55). Light yellow solid, yield 83%. R_f = 0.67 (10% MeOH in DCM). Mp 68–70 °C. $[\alpha]_D^{20}$ = −16.00. ^{1}H NMR (400 MHz, $CDCl_3$) δ: 8.75 (s, 1H), 7.55 (d, J = 7.7 Hz, 1H), 7.38 (d, J = 7.6 Hz, 1H), 7.19–6.99 (m, 7H), 6.56 (s, 1H), 5.98 (brs, 1H), 5.29–5.26 (m, 1H), 5.13–5.09 (m, 2H), 4.66–4.56 (m, 3H), 4.40–4.34 (m, 2H), 3.25–3.19 (m, 2H), 2.95–2.84 (m, 2H), 2.33 (s, 3H), 1.44 (s, 9H). ^{13}C NMR (75 MHz, $CDCl_3$) δ: 172.13, 169.44, 155.24, 142.42, 141.22, 137.35, 136.09, 134.58, 129.39, 127.75, 125.01, 123.32, 121.90, 119.44, 118.76, 111.37, 109.36, 79.97, 58.23, 54.54, 46.11, 43.49, 35.63, 28.35, 28.06, 21.07. IR ν_{max} (neat)/cm^{-1} 3089 (CH), 1514 (C═C) and 1462 (N═N). MS (ESI), m/z: 559.15 $[M - H]^-$, 561.65 $[M + H]^+$.

(*R*)-(1-(3-(4-Methoxybenzylamino)-3-oxopropyl)-1*H*-1,2,3-triazol-4-yl)methyl 2-[(*tert*-butoxycarbonyl)amino]-3-phenylpropanoate (56). Creamish solid, yield 95%. R_f = 0.76 (10% MeOH in DCM). Mp 108–110 °C. $[\alpha]_D^{20}$ = −16.00. ^{1}H NMR (400 MHz, $CDCl_3$) δ: 7.60 (s, 1H), 7.24–7.22 (m, 3H), 7.10 (d, J = 8.5 Hz,

2H), 7.06–7.04 (m, 2H), 6.84 (d, J = 8.5 Hz, 2H), 5.79 (brs, 1H), 5.22 (s, 2H), 4.95 (d, J = 7.8 Hz, 1H), 4.74–4.67 (m, 2H), 4.55–4.53 (m, 1H), 4.31 (d, J = 5.6 Hz, 2H), 3.78 (s, 3H), 3.11–2.99 (m, 2H), 2.83 (t, J = 6.2 Hz, 2H), 1.40 (s, 9H). ^{13}C NMR (75 MHz, $CDCl_3$) δ: 171.64, 168.82, 159.09, 155.09, 142.08, 135.83, 129.82, 129.34, 129.11, 128.50, 126.99, 125.06, 114.09, 80.02, 58.26, 55.29, 54.39, 46.23, 43.19, 38.04, 36.36, 28.27. IR ν_{max} (neat)/cm^{-1} 3070 (CH), 1514 (C=C) and 1458 (N=N). MS (ESI), m/z: 538.1 $[M + H]^+$.

(*R*)-(1-(3-(4-Methoxybenzylamino)-3-oxopropyl)-1*H*-1,2,3-triazol-4-yl)methyl 1-(*tert*-butoxycarbonyl)pyrrolidine-2-carboxylate (57). Light yellow oil, yield 86%. R_f = 0.71 (10% MeOH in DCM). $[\alpha]_D^{20}$ = −44.00. ^{1}H NMR (400 MHz, $CDCl_3$) δ: 7.69 (d, J = 4.5 Hz, 1H), 7.16–7.08 (m, 2H), 6.86–6.83 (m, 2H), 6.10 (brs, 1H), 5.26–5.21 (m, 2H), 4.73–4.66 (m, 2H), 4.33–4.32 (m, 2H), 4.24–4.12 (m, 1H), 3.79 (s, 3H), 3.52–3.45 (m, 2H), 2.86–2.78 (m, 2H), 1.96–1.82 (m, 2H), 1.70 (m, 2H), 1.43 (s, 9H). ^{13}C NMR (75 MHz, $CDCl_3$) δ: 173.03, 168.89, 159.10, 154.42, 142.92, 129.95, 129.11, 124.97, 114.08, 79.92, 58.99, 58.12, 55.29, 46.63, 43.17, 36.59, 30.79, 29.78, 28.41, 24.34. IR ν_{max} (neat)/cm^{-1} 3095 (CH), 1514 (C=C) and 1462 (N=N). MS (ESI), m/z: 388.2 $[M + H - Boc]^+$, 488.08 $[M + H]^+$.

(*R*)-(1-(3-(4-Methoxybenzylamino)-3-oxopropyl)-1*H*-1,2,3-triazol-4-yl)methyl 2-[(*tert*-butoxycarbonyl)amino]-3-(1*H*-indol-3-yl)propanoate (58). Light yellow solid, yield 92%. R_f = 0.67 (10% MeOH in DCM). Mp 72–74 °C. $[\alpha]_D^{20}$ = −20.00. ^{1}H NMR (400 MHz, $CDCl_3$) δ: 8.84 (s, 1H), 7.55 (d, J = 7.8 Hz, 1H), 7.38 (d, J = 8.0 Hz, 1H), 7.19–7.15 (m, 2H), 7.10–7.07 (m, 3H), 6.83 (d, J = 8.6 Hz, 2H), 6.52 (s, 1H), 6.02 (brs, 1H), 5.29–5.26 (m, 1H), 5.12–5.09 (m, 2H), 4.67–4.52 (m, 3H), 4.34–4.30 (m, 2H), 3.78 (s, 3H), 3.26–3.20 (m, 2H), 2.96–2.83 (m, 2H), 1.44 (s, 9H). ^{13}C NMR (75 MHz, $CDCl_3$) δ: 172.12, 169.36, 159.07, 155.24, 142.43, 136.09, 129.66, 128.93, 127.76, 125.00, 123.31, 121.91, 119.44, 118.76, 114.10, 111.35, 109.39, 79.95, 58.23, 55.29, 54.54, 46.10, 43.23, 35.61, 28.35, 28.02. IR ν_{max} (neat)/cm^{-1} 3067 (CH), 1514 (C=C) and 1460 (N=N). MS (ESI), m/z: 575.37 $[M - H]^-$, 577.10 $[M + H]^+$.

(*R*)-(1-(3-(4-Trifluoromethylbenzylamino)-3-oxopropyl)-1*H*-1,2,3-triazol-4-yl)methyl 2-[(*tert*-butoxycarbonyl)amino]-3-phenylpropanoate (59). White solid, yield 94%. R_f = 0.53 (10% MeOH in DCM). Mp 103–105 °C. $[\alpha]_D^{20}$ = −20.00. ^{1}H NMR (400 MHz, $CDCl_3$) δ: 7.57–7.55 (m, 3H), 7.33–7.22 (m, 4H), 7.05–7.04 (m, 2H), 6.19 (brs, 1H), 5.22 (s, 2H), 4.94 (d, J = 7.2 Hz, 1H), 4.75–4.68 (m, 2H), 4.49–4.47 (m, 1H), 4.43 (d, J = 5.7 Hz, 2H), 3.09–2.98 (m, 2H), 2.89 (brs, 2H), 1.39 (s, 9H). ^{13}C NMR (75 MHz, $CDCl_3$) δ: 171.68, 169.22, 155.14, 142.24, 141.96, 135.76, 129.30, 128.53, 127.82, 127.04, 125.62, 125.57, 125.09, 80.09, 58.19, 54.43, 46.23, 43.11, 37.96, 36.27, 28.26. IR ν_{max} (neat)/cm^{-1} 3032 (CH), 1529 (C=C) and 1447 (N=N). MS (ESI), m/z: 576.1 $[M + H]^+$.

(*R*)-(1-(3-(4-Trifluoromethylbenzylamino)-3-oxopropyl)-1*H*-1,2,3-triazol-4-yl)methyl 1-(*tert*-butoxycarbonyl)pyrrolidine-2-carboxylate (60). Colorless oil, yield 94%. R_f = 0.48 (10% MeOH in DCM). $[\alpha]_D^{20}$ = −40.00. ^{1}H NMR (300 MHz, $CDCl_3$) δ: 7.52 (d, J = 7.8 Hz, 1H), 7.35–7.07 (m, 4H), 6.76 (brs, 1H), 5.29–5.05 (m, 2H), 4.61–4.56 (m, 2H), 4.53 (d, J = 6.0 Hz, 2H), 4.25–4.16 (m, 1H), 3.21 (brs, 2H), 3.03–2.86 (m, 2H), 2.21–2.15 (m, 1H), 1.94–1.86 (m, 3H), 1.42 (s, 9H). ^{13}C NMR (75 MHz, $CDCl_3$) δ: 172.12, 169.72, 155.27, 142.58, 136.06, 127.65, 125.61, 123.18, 119.50, 111.29, 80.01, 58.16, 54.48, 46.09, 43.14, 35.51, 29.70, 28.32, 27.91. IR ν_{max} (neat)/cm^{-1} 3082 (CH), 1546 (C=C) and 1452 (N=N). MS (ESI), m/z: 426.05 $[M + H - Boc]^+$, 526.04 $[M + H]^+$.

(*R*)-(1-(3-(4-Trifluoromethylbenzylamino)-3-oxopropyl)-1*H*-1,2,3-triazol-4-yl)methyl 2-[(*tert*-butoxycarbonyl)amino]-3-(1*H*-indol-3-yl)propanoate (61). Light yellow solid, yield 76%. R_f = 0.47 (10% MeOH in DCM). Mp 55–60 °C. $[\alpha]_D^{20}$ = −20.00. ^{1}H NMR (400 MHz, $CDCl_3$) δ: 8.71 (s, 1H), 7.54 (t, J = 8.0 Hz, 3H), 7.35 (d, J = 8.1 Hz, 1H), 7.24–7.14 (m, 3H), 7.08 (t, J = 7.4 Hz, 2H), 6.50 (s, 1H), 6.28 (brs, 1H), 5.29–5.26 (m, 1H), 5.14–5.09 (m, 2H), 4.63–4.52 (m, 3H), 4.43 (s, 2H), 3.23 (s, 2H), 2.99–2.88 (m, 2H), 1.43 (s, 9H). ^{13}C NMR (75 MHz, $CDCl_3$) δ: 172.99, 169.43, 154.47, 153.76, 143.02, 142.26, 137.93, 136.29, 127.79, 126.04, 125.47, 125.08, 124.50, 121.87, 119.23, 118.45, 111.21, 109.34, 79.98, 58.96, 57.99, 46.66, 42.99, 36.54, 30.72, 28.37. IR ν_{max} (neat)/cm^{-1} 3091 (CH), 1510 (C=C) and 1460 (N=N). MS (ESI), m/z: 613.27 $[M - H]^-$, 615.13 $[M + H]^+$.

(*R*)-(1-(3-(4-Trifluoromethoxybenzylamino)-3-oxopropyl)-1*H*-1,2,3-triazol-4-yl)methyl 2-[(*tert*-butoxycarbonyl)amino]-3-phenylpropanoate (62). Light yellow solid, yield 89%. R_f = 0.69 (10% MeOH in DCM). Mp 110–113 °C. $[\alpha]_D^{20}$ = −24.00. ^{1}H NMR (300 MHz, $CDCl_3$) δ: 7.49 (s, 1H), 7.28–7.21 (m, 5H), 7.09–6.89 (m, 4H), 5.91 (brs, 1H), 5.23 (s, 2H), 4.67 (d, J = 7.4 Hz, 1H), 4.71 (t, J = 5.8 Hz, 2H), 4.48–4.46 (m, 1H), 4.41 (d, J = 5.4 Hz, 2H), 3.12–3.01 (m, 2H), 2.82 (t, J = 6.8 Hz, 2H), 1.40 (s, 9H). ^{13}C NMR (75 MHz, $CDCl_3$) δ: 171.82, 169.78, 156.24, 142.63, 137.89, 137.09, 135.86, 128.54, 127.61, 127.32, 124.78, 123.29, 121.56, 115.45, 79.32, 58.51, 54.71, 46.31, 43.71, 38.67, 35.55, 28.35. IR ν_{max} (neat)/cm^{-1} 3067 (CH), 1533 (C=C) and 1447 (N=N). MS (ESI), m/z: 592.3 $[M + H]^+$.

(*R*)-(1-(3-(4-Trifluoromethoxybenzylamino)-3-oxopropyl)-1*H*-1,2,3-triazol-4-yl)methyl 1-(*tert*-butoxycarbonyl)pyrrolidine-2-carboxylate (63). Light yellow oil, yield 89%. R_f = 0.65 (10% MeOH in DCM). $[\alpha]_D^{20}$ = −44.00. ^{1}H NMR (300 MHz, $CDCl_3$) δ: 7.71 (d, J = 9.7 Hz, 1H), 7.24–7.16 (m, 2H), 7.02–6.95 (m, 2H), 6.43 (brs, 1H), 5.41–5.28 (m, 2H), 4.75–4.68 (m, 2H), 4.42–4.39 (m, 2H), 4.28–4.25 (m, 1H), 3.67–3.47 (m, 2H), 2.81–2.76 (m, 2H), 2.12–1.89 (m, 4H), 1.39–1.32 (m, 9H). ^{13}C NMR (75 MHz, $CDCl_3$) δ: 173.12, 168.12, 158.23, 154.30, 142.73, 139.32, 135.03, 129.02, 124.82, 121.67, 114.23, 79.78, 58.23, 46.85, 46.30, 42.80, 35.67, 30.56, 28.23, 23.70. IR ν_{max} (neat)/cm^{-1} 3056 (CH), 1544 (C=C) and 1460 (N=N). MS (ESI), m/z: 542.3 $[M + H]^+$.

(*R*)-(1-(3-(4-Trifluoromethoxybenzylamino)-3-oxopropyl)-1*H*-1,2,3-triazol-4-yl)methyl 2-(*tert*-butoxycarbonyl)-3-(1*H*-indol-3-yl)propanoate (64). Light yellow solid, yield 89%. R_f = 0.62 (10% MeOH in DCM). Mp 70–72 °C. $[\alpha]_D^{20}$ = −24.00. ^{1}H NMR (300 MHz, $CDCl_3$) δ: 8.92 (s, 1H), 7.56 (d, J = 7.0 Hz, 1H), 7.32–7.28 (m, 4H), 7.14–7.02 (m, 5H), 6.43 (s, 1H), 6.21 (brs, 1H), 5.46–5.41 (m, 1H), 5.14–5.03 (m, 2H), 4.65–4.51 (m, 3H), 4.23 (m, 2H), 3.19–3.12 (m, 2H), 2.87–2.72 (m, 2H), 1.43 (s, 9H). ^{13}C NMR (75 MHz, $CDCl_3$) δ: 171.88, 169.57, 156.12,

142.87, 137.51, 136.24, 128.54, 127.78, 127.21, 124.73, 122.89, 121.72, 119.03, 118.56, 111.47, 109.25, 79.89, 58.21, 54.76, 46.23, 43.53, 36.03, 28.42. IR ν_{max} (neat)/cm^{-1} 3078 (CH), 1510 (C=C) and 1460 (N=N). MS (ESI), *m*/*z*: 630.1 $[M + H]^+$.

Deprotection of boc-protected triazole–amino acid hybrids (65–88). Example: synthesis of (*R*)-(1-(3-(4-fluorobenzylamino)-3-oxopropyl)-1*H*-1,2,3-triazol-4-yl)methyl 2-amino-3-phenylpropanoate (68)

Compound **44** (0.57 mmol, 0.3 g) was dissolved in dichloromethane (10 mL). To this solution *p*-toluene sulphonic acid (*p*TSA) (1.71 mmol, 0.32 g) was added. The reaction was stirred for 3 h at room temperature. After completion of the reaction, it was neutralized by using sat. sodium bicarbonate solution and the compound was extracted by ethyl acetate, washed with water and brine to get final compound (**68**).

(*R*)-(1-(3-(Benzylamino)-3-oxopropyl)-1*H*-1,2,3-triazol-4-yl)methyl 2-amino-3-phenylpropanoate (65). Yellow solid, yield 85%. R_f = 0.69 (10% MeOH in DCM). Mp 165–167 °C. ^{1}H NMR (400 MHz, DMSO-d_6) δ: 7.86 (s, 1H), 7.29–7.15 (m, 10H), 6.68 (brs, 1H), 5.17 (s, 2H), 4.57 (t, *J* = 6.7 Hz, 2H), 4.49 (s, 2H), 4.25 (d, *J* = 5.6 Hz, 2H), 3.63–3.60 (m, 1H), 3.17–3.12 (m, 2H), 2.79 (t, *J* = 7.3 Hz, 2H). ^{13}C NMR (75 MHz, $CDCl_3$) δ: 173.89, 169.13, 162.49, 142.56, 137.85, 133.70, 129.54, 128.68, 127.69, 127.31, 126.85, 123.08, 57.28, 55.91, 46.19, 43.63, 40.65, 36.42. IR ν_{max} (neat)/cm^{-1} 3290 (NH_2) and 3070 (CH). MS (ESI), *m*/*z*: 408.2 $[M + H]^+$.

(*R*)-(1-(3-(Benzylamino)-3-oxopropyl)-1*H*-1,2,3-triazol-4-yl)methyl pyrrolidine-2-carboxylate (66). Yellow oil, yield 89%. R_f = 0.33 (10% MeOH in DCM). ^{1}H NMR (300 MHz, DMSO-d_6) δ: 8.51 (brs, 1H), 7.87 (s, 1H), 7.32–7.15 (m, 5H), 5.14 (brs, 1H), 4.58 (t, *J* = 6.9 Hz, 2H), 4.50 (s, 2H), 4.26 (d, *J* = 5.7 Hz, 2H), 3.64–3.59 (m, 1H), 3.23–3.17 (m, 2H), 2.78 (t, *J* = 6.6 Hz, 2H), 2.01–1.91 (m, 2H), 1.72–1.65 (m, 2H). ^{13}C NMR (75 MHz, $CDCl_3$) δ: 173.24, 169.35, 148.04, 138.37, 128.39, 127.59, 127.11, 122.66, 60.03, 56.07, 46.12, 43.20, 36.20, 30.78, 29.54, 24.32. IR ν_{max} (neat)/cm^{-1} 3290 (NH_2) and 3070 (CH). MS (ESI), *m*/*z*: 358.6 $[M + H]^+$.

(*R*)-(1-(3-(Benzylamino)-3-oxopropyl)-1*H*-1,2,3-triazol-4-yl)methyl 2-amino-3-(1*H*-indol-3-yl)propanoate (67). Yellow oil, yield 88%. R_f = 0.41 (10% MeOH in DCM). ^{1}H NMR (300 MHz, $CDCl_3$) δ: 8.96 (s, 1H), 7.48 (d, *J* = 7.5 Hz, 1H), 7.28 (d, *J* = 7.8 Hz, 1H), 7.19–6.96 (m, 8H), 6.74 (brs, 1H), 6.66 (s, 1H), 5.13–4.97 (m, 2H), 4.59–4.46 (m, 2H), 4.27 (d, *J* = 5.4 Hz, 2H), 3.75 (t, *J* = 6.0 Hz, 1H), 3.07–3.04 (m, 1H), 2.78–2.70 (m, 3H). ^{13}C NMR (75 MHz, $CDCl_3$) δ: 174.98, 169.45, 142.46, 137.78, 136.22, 133.67, 128.67, 127.52, 124.81, 123.38, 121.88, 119.35, 118.70, 111.37, 110.13, 57.94, 55.16, 46.14, 43.62, 35.83, 30.41. IR ν_{max} (neat)/cm^{-1} 3391 (NH_2) and 3068 (CH). MS (ESI), *m*/*z*: 445.0 $[M - H]^-$, 447.0 $[M + H]^+$.

(*R*)-(1-(3-(4-Fluorobenzylamino)-3-oxopropyl)-1*H*-1,2,3-triazol-4-yl)methyl 2-amino-3-phenylpropanoate (68). Creamish solid, yield 85%. R_f = 0.67 (10% MeOH in DCM). Mp 184–186 °C. ^{1}H NMR (300 MHz, $CDCl_3$) δ: 7.51 (s, 1H), 7.21–7.16 (m, 3H), 7.08–7.03 (m, 4H), 6.89 (t, *J* = 8.7 Hz, 2H), 6.52 (brs, 1H), 5.09 (s, 2H), 4.57 (t, *J* = 5.6 Hz, 2H), 4.26 (d, *J* = 5.4 Hz, 2H), 3.66–3.62 (m, 1H), 2.99–2.93 (m, 1H), 2.81–2.72 (m, 3H). ^{13}C NMR (75 MHz, $CDCl_3$) δ: 174.59, 169.07, 160.52, 142.28, 136.92, 133.70, 129.41, 129.30, 128.54, 126.85, 125.03, 115.65, 57.84, 55.66, 46.19, 42.91, 40.89, 36.16. IR ν_{max} (neat)/cm^{-1} 3283 (NH_2) and 3074 (CH). MS (ESI), *m*/*z*: 426.2 $[M + H]^+$.

(*R*)-(1-(3-(4-Fluorobenzylamino)-3-oxopropyl)-1*H*-1,2,3-triazol-4-yl)methyl pyrrolidine-2-carboxylate (69). Light yellow solid, yield 89%. R_f = 0.33 (10% MeOH in DCM). Mp = 70–76 °C. ^{1}H NMR (400 MHz, $CDCl_3$) δ: 7.60 (s, 1H), 7.16–7.13 (m, 2H), 7.02–6.98 (m, 2H), 5.94 (brs, 1H), 4.75 (s, 2H), 4.70 (t, *J* = 6.1 Hz, 2H), 4.36 (d, *J* = 5.8 Hz, 2H), 3.62–3.57 (m, 1H), 3.12–3.03 (m, 2H), 2.86 (t, *J* = 6.2 Hz, 2H), 2.23–2.07 (m, 2H), 1.86–1.74 (m, 2H). ^{13}C NMR (75 MHz, $CDCl_3$) δ: 173.98, 169.40, 160.25, 148.02, 134.24, 129.31, 127.74, 126.89, 122.70, 115.31, 56.09, 46.12, 42.49, 36.21, 29.53, 24.46. IR ν_{max} (neat)/cm^{-1} 3290 (NH_2) and 3070 (CH). MS (ESI), *m*/*z*: 376.0 $[M + H]^+$.

(*R*)-(1-(3-(4-Fluorobenzylamino)-3-oxopropyl)-1*H*-1,2,3-triazol-4-yl)methyl 2-amino-3-(1*H*-indol-3-yl)propanoate (70). Yellow oil, yield 90%. R_f = 0.41 (10% MeOH in DCM). ^{1}H NMR (300 MHz, $CDCl_3$) δ: 8.81 (s, 1H), 7.48 (d, *J* = 7.8 Hz, 1H), 7.27 (d, *J* = 8.1 Hz, 1H), 7.11–6.98 (m, 5H), 6.87 (t, *J* = 8.2 Hz, 2H), 6.64–6.58 (m, 2H), 5.14–4.96 (m, 2H), 4.54–4.42 (m, 2H), 4.22 (d, *J* = 5.7 Hz, 2H), 3.74 (t, *J* = 6.0 Hz, 1H), 3.11–3.00 (m, 2H), 2.84–2.77 (m, 2H). ^{13}C NMR (75 MHz, $CDCl_3$) δ: 175.13, 169.42, 142.56, 136.19, 133.53, 129.27, 127.64, 124.88, 123.23, 121.94, 119.41, 118.76, 115.66, 111.32, 110.33, 57.85, 55.23, 46.09, 42.92, 35.73, 30.53. IR ν_{max} (neat)/cm^{-1} 3272 (NH_2) and 3074 (CH). MS (ESI), *m*/*z*: 463.0 $[M - H]^-$, 465.2 $[M + H]^+$.

(*R*)-(1-(3-(4-Chlorobenzylamino)-3-oxopropyl)-1*H*-1,2,3-triazol-4-yl)methyl 2-amino-3-phenylpropanoate (71). Creamish solid, yield 88%. R_f = 0.43 (10% MeOH in DCM). Mp 120–122 °C. ^{1}H NMR (400 MHz, DMSO-d_6) δ: 7.97 (s, 1H), 7.34 (d, *J* = 8.2 Hz, 2H), 7.28–7.12 (m, 7H), 6.92–6.88 (m, 1H), 5.18–5.10 (m, 2H), 4.61–4.55 (m, 2H), 4.49 (s, 2H), 4.24–4.23 (m, 2H), 3.61–3.58 (m, 1H), 2.88–2.77 (m, 4H). ^{13}C NMR (75 MHz, $CDCl_3$) δ: 173.66, 169.09, 157.13, 142.17, 136.45, 133.32, 129.31, 128.78, 128.52, 127.01, 125.07, 124.24, 58.20, 54.43, 46.25, 42.93, 40.92, 36.26. IR ν_{max} (neat)/cm^{-1} 3294 (NH_2) and 3070 (CH). MS (ESI), *m*/*z*: 442.0 $[M + H]^+$.

(*R*)-(1-(3-(4-Chlorobenzylamino)-3-oxopropyl)-1*H*-1,2,3-triazol-4-yl)methyl pyrrolidine-2-carboxylate (72). Yellow oil, yield 90%. R_f = 0.37 (10% MeOH in DCM). ^{1}H NMR (300 MHz, $CDCl_3$) δ: 8.55 (s, 1H), 7.86 (s, 1H), 7.35 (d, *J* = 8.4 Hz, 2H), 7.17 (d, *J* = 8.4 Hz, 2H), 5.16 (brs, 1H), 4.57 (t, *J* = 6.8 Hz, 2H), 4.49 (s, 2H), 4.24 (d, *J* = 6.0 Hz, 2H), 3.65–3.60 (m, 2H), 3.04–2.98 (m, 1H), 2.78 (t, *J* = 6.8 Hz, 2H), 2.01–1.89 (m, 2H), 1.78–1.67 (m, 2H). ^{13}C NMR (75 MHz, $CDCl_3$) δ: 172.24, 169.18, 148.20, 138.78, 128.92, 127.67, 127.42, 122.02, 61.24, 56.29, 46.23, 42.84, 36.28, 31.83, 29.56, 24.56. IR ν_{max} (neat)/cm^{-1} 3284 (NH_2) and 3078 (CH). MS (ESI), *m*/*z*: 392.0 $[M + H]^+$.

(*R*)-(1-(3-(4-Chlorobenzylamino)-3-oxopropyl)-1*H*-1,2,3-triazol-4-yl)methyl 2-amino-3-(1*H*-indol-3-yl)propanoate (73). Yellow oil, yield 87%. R_f = 0.67 (10% MeOH in DCM). ^{1}H NMR (400 MHz, $CDCl_3$) δ: 8.57 (s, 1H), 7.59 (d, *J* = 7.3 Hz, 1H), 7.37 (d, *J* = 7.9 Hz, 1H), 7.28 (brs, 2H), 7.19–7.11 (m, 2H), 7.15–7.07 (m, 3H), 6.68 (s, 1H), 5.95 (brs, 1H), 5.29–5.10 (m, 2H),

4.63–4.58 (m, 2H), 4.35–4.34 (m, 2H), 3.87 (t, J = 6.1 Hz, 1H), 3.17–3.15 (m, 2H), 2.95–2.85 (m, 2H). ^{13}C NMR (75 MHz, $CDCl_3$) δ: 174.39, 169.56, 142.32, 136.78, 133.54, 128.74, 128.51, 127.72, 125.31, 123.24, 121.63, 119.39, 118.43, 111.33, 109.45, 58.01, 54.23, 46.57, 42.81, 35.76, 30.42. IR ν_{max} (neat)/cm^{-1} 3264 (NH_2) and 3063 (CH). MS (ESI), m/z: 479.0 $[M - H]^-$, 481.2 $[M + H]^+$.

(*R*)-(1-(3-(2-Chlorobenzylamino)-3-oxopropyl)-1*H*-1,2,3-triazol-4-yl)methyl 2-amino-3-phenylpropanoate (74). Yellow oil, yield 84%. R_f = 0.53 (10% MeOH in DCM). ^{1}H NMR (300 MHz, $CDCl_3$) δ: 7.49 (s, 1H), 7.24–7.19 (m, 5H), 7.04–6.99 (m, 4H), 6.58 (brs, 1H), 5.20 (s, 2H), 4.58 (t, J = 6.2 Hz, 2H), 4.38 (s, 2H), 4.20–4.16 (m, 2H), 3.72–3.68 (m, 1H), 3.01–2.76 (m, 4H). ^{13}C NMR (75 MHz, $CDCl_3$) δ: 174.32, 169.40, 161.23, 147.45, 135.18, 133.49, 129.87, 129.52, 128.99, 128.26, 127.06, 125.91, 123.05, 56.09, 54.23, 46.14, 43.24, 41.56, 36.29. IR ν_{max} (neat)/cm^{-1} 3279 (NH_2) and 3067 (CH). MS (ESI), m/z: 442.2 $[M + H]^+$.

(*R*)-(1-(3-(2-Chlorobenzylamino)-3-oxopropyl)-1*H*-1,2,3-triazol-4-yl)methyl pyrrolidine-2-carboxylate (75). Yellow oil, yield 92%. R_f = 0.35 (10% MeOH in DCM). ^{1}H NMR (300 MHz, $CDCl_3$) δ: 8.55 (brs, 1H), 7.87 (s, 1H), 7.44–7.41 (m, 1H), 7.31–7.27 (m, 2H), 7.17–7.14 (m, 1H), 5.14 (brs, 1H), 4.58 (t, J = 6.8 Hz, 2H), 4.50 (s, 2H), 4.31 (d, J = 6.6 Hz, 2H), 3.78–3.62 (m, 1H), 3.21–3.14 (m, 2H), 2.83 (t, J = 6.6 Hz, 2H), 2.11–2.02 (m, 1H), 1.95–1.84 (m, 3H). ^{13}C NMR (75 MHz, $CDCl_3$) δ: 173.42, 169.44, 147.49, 135.22, 133.46, 129.81, 129.50, 128.96, 128.43, 127.05, 123.02, 60.23, 56.09, 46.16, 41.53, 36.29, 29.69, 24.56. IR ν_{max} (neat)/cm^{-1} 3279 (NH_2) and 3074 (CH). MS (ESI), m/z: 392.0 $[M + H]^+$.

(*R*)-(1-(3-(2-Chlorobenzylamino)-3-oxopropyl)-1*H*-1,2,3-triazol-4-yl)methyl 2-amino-3-(1*H*-indol-3-yl)propanoate (76). Yellow oil, yield 82%. R_f = 0.50 (10% MeOH in DCM). ^{1}H NMR (300 MHz, $CDCl_3$) δ: 8.83 (s, 1H), 7.47 (brs, 1H), 7.29–6.96 (m, 8H), 6.68 (s, 1H), 6.59 (s, 1H), 5.16–4.97 (m, 2H), 4.58 (s, 2H), 4.53 (t, J = 6.3 Hz, 2H), 4.36 (d, J = 5.4 Hz, 2H), 3.08–3.06 (m, 1H), 2.80–2.72 (m, 3H). ^{13}C NMR (75 MHz, $CDCl_3$) δ: 174.65, 169.52, 147.43, 142.39, 135.14, 133.49, 129.89, 129.53, 129.02, 127.06, 124.89, 123.03, 121.95, 119.44, 118.68, 111.36, 109.95, 57.96, 56.04, 46.12, 41.58, 36.25, 29.68. IR ν_{max} (neat)/cm^{-1} 3260 (NH_2) and 3063 (CH). MS (ESI), m/z: 479.0 $[M - H]^-$, 481.2 $[M + H]^+$.

(*R*)-(1-(3-(4-Methylbenzylamino)-3-oxopropyl)-1*H*-1,2,3-triazol-4-yl)methyl 2-amino-3-phenylpropanoate (77). Light yellow solid, yield 89%. R_f = 0.50 (10% MeOH in DCM). Mp 168–170 °C. ^{1}H NMR (300 MHz, $CDCl_3$) δ: 7.52 (d, J = 10.8 Hz, 1H), 7.19–6.98 (m, 9H), 6.54–6.36 (m, 1H), 5.09 (s, 2H), 4.58–4.54 (m, 2H), 4.24 (s, 2H), 3.66 (brs, 1H), 2.81–2.74 (m, 2H), 2.47 (brs, 2H), 2.23 (s, 3H). ^{13}C NMR (75 MHz, $CDCl_3$) δ: 174.38, 169.17, 147.49, 142.19, 137.28, 134.79, 129.33, 128.56, 127.70, 126.88, 125.06, 123.03, 57.94, 55.59, 46.21, 43.43, 40.66, 36.43, 21.07. IR ν_{max} (neat)/cm^{-1} 3298 (NH_2) and 3067 (CH). MS (ESI), m/z: 422.2 $[M + H]^+$.

(*R*)-(1-(3-(4-Methylbenzylamino)-3-oxopropyl)-1*H*-1,2,3-triazol-4-yl)methyl pyrrolidine-2-carboxylate (78). Light yellow solid, yield 83%. R_f = 0.26 (10% MeOH in DCM). Mp 109–111 °C. ^{1}H NMR (300 MHz, $CDCl_3$) δ: 8.43 (brs, 1H), 7.85 (s, 1H), 7.11–7.04 (m, 4H), 4.57 (t, J = 6.8 Hz, 2H), 4.50 (s, 2H), 4.21 (d, J = 5.7 Hz, 2H), 3.68–3.63 (m, 1H), 3.19–2.94 (m, 2H), 2.77 (t, J = 5.7 Hz, 2H), 2.29 (s, 3H), 1.99–1.90 (m, 2H), 1.71–1.64 (m, 2H). ^{13}C NMR (75 MHz, $CDCl_3$) δ: 172.10, 169.42, 148.27, 136.58, 136.26, 129.25, 128.56, 127.63, 123.25, 59.61, 55.51, 46.14, 42.92, 35.99, 30.65, 29.38, 21.11. IR ν_{max} (neat)/cm^{-1} 3294 (NH_2) and 3074 (CH). MS (ESI), m/z: 372.2 $[M + H]^+$.

(*R*)-(1-(3-(4-Methylbenzylamino)-3-oxopropyl)-1*H*-1,2,3-triazol-4-yl)methyl 2-amino-3-(1*H*-indol-3-yl)propanoate (79). Yellow oil, yield 85%. R_f = 0.50 (10% MeOH in DCM). ^{1}H NMR (300 MHz, $CDCl_3$) δ: 8.63 (s, 1H), 7.52 (brs, 1H), 7.32–6.97 (m, 8H), 6.64 (s, 1H), 5.99–5.91 (m, 1H), 5.19–5.00 (m, 2H), 4.65–4.51 (m, 2H), 4.27–4.25 (m, 2H), 3.79 (brs, 1H), 3.09–3.08 (m, 1H), 2.79–2.74 (m, 3H), 2.25 (s, 3H). ^{13}C NMR (75 MHz, $CDCl_3$) δ: 174.89, 169.76, 142.41, 137.54, 136.38, 133.45, 129.54, 128.32, 127.43, 125.21, 123.67, 121.83, 119.75, 118.32, 111.63, 109.23, 58.42, 54.61, 46.21, 43.68, 35.42, 28.35, 21.07. IR ν_{max} (neat)/cm^{-1} 3279 (NH_2) and 3059 (CH). MS (ESI), m/z: 459.2 $[M - H]^-$, 461.2 $[M + H]^+$, 483.2 $[M + Na]^+$.

(*R*)-(1-(3-(4-Methoxybenzylamino)-3-oxopropyl)-1*H*-1,2,3-triazol-4-yl)methyl 2-amino-3-phenylpropanoate (80). Light yellow solid, yield 87%. R_f = 0.57 (10% MeOH in DCM). Mp 168–170 °C. ^{1}H NMR (400 MHz, DMSO-d_6) δ: 7.85 (s, 1H), 7.30–7.18 (m, 4H), 7.14–7.08 (m, 3H), 6.86–6.83 (m, 2H), 6.68–6.65 (m, 1H), 5.09 (s, 2H), 4.60–4.54 (m, 2H), 4.49 (s, 2H), 4.18 (d, J = 5.6 Hz, 2H), 3.72 (s, 3H), 3.58–3.56 (m, 1H), 2.85–2.73 (m, 4H). ^{13}C NMR (75 MHz, $CDCl_3$) δ: 173.65, 168.78, 158.43, 142.38, 137.61, 133.83, 129.11, 128.64, 126.90, 125.11, 122.93, 56.35, 55.30, 52.39, 46.22, 43.24, 40.43, 36.36. IR ν_{max} (neat)/cm^{-1} 3286 (NH_2) and 3070 (CH). MS (ESI), m/z: 436.5 $[M - H]^-$, 438.1 $[M + H]^+$.

(*R*)-(1-(3-(4-Methoxybenzylamino)-3-oxopropyl)-1*H*-1,2,3-triazol-4-yl)methylpyrrolidine-2-carboxylate (81). Yellow solid, yield 90%. R_f = 0.14 (10% MeOH in DCM). ^{1}H NMR (300 MHz, $CDCl_3$) δ: 8.46 (brs, 1H), 7.86 (s, 1H), 7.09 (d, J = 8.4 Hz, 2H), 6.85 (d, J = 8.4 Hz, 2H), 4.57 (t, J = 6.8 Hz, 2H), 4.50 (s, 2H), 4.18 (d, J = 5.7 Hz, 2H), 3.72 (s, 3H), 3.69–3.64 (m, 1H), 3.42–3.37 (m, 2H), 2.76 (t, J = 7.0 Hz, 2H), 1.96–1.91 (m, 2H), 1.78–1.65 (m, 2H). ^{13}C NMR (75 MHz, $CDCl_3$) δ: 173.65, 169.36, 148.26, 138.37, 131.56, 128.98, 123.26, 114.21, 61.19, 57.23, 55.51, 46.15, 42.00, 36.01, 30.63, 29.37, 24.31. IR ν_{max} (neat)/cm^{-1} 3290 (NH_2) and 3074 (CH). MS (ESI), m/z: 388.2 $[M + H]^+$.

(*R*)-(1-(3-(4-Methoxybenzylamino)-3-oxopropyl)-1*H*-1,2,3-triazol-4-yl)methyl 2-amino-3-(1*H*-indol-3-yl)propanoate (82). Yellow solid, yield 89%. R_f = 0.53 (10% MeOH in DCM). Mp 150–154 °C. ^{1}H NMR (400 MHz, $CDCl_3$) δ: 8.41 (s, 1H), 7.91 (s, 1H), 7.48 (d, J = 7.8 Hz, 1H), 7.32 (d, J = 7.9 Hz, 1H), 7.09–7.06 (m, 5H), 6.96 (t, J = 7.4 Hz, 1H), 6.89 (m, 2H), 5.06 (s, 2H), 4.57 (t, J = 6.4 Hz, 2H), 4.17 (d, J = 5.6 Hz, 2H), 3.71 (s, 3H), 3.66–3.63 (m, 1H), 3.03–2.89 (m, 2H), 2.76 (t, J = 6.5 Hz, 2H). ^{13}C NMR (75 MHz, $CDCl_3$) δ: 173.12, 169.45, 142.79, 136.32, 133.59, 129.54, 128.43, 127.61, 125.51, 123.21, 121.87, 119.37, 118.63, 114.21, 111.53, 109.25, 58.53, 55.21, 54.76, 46.62, 43.38, 35.54, 30.56. IR ν_{max} (neat)/cm^{-1} 3279 (NH_2) and 3082 (CH). MS (ESI), m/z: 475.2 $[M - H]^-$, 477.2 $[M + H]^+$.

(*R*)-(1-(3-(4-(Trifluoromethyl)benzylamino)-3-oxopropyl)-1*H*-1,2,3-triazol-4-yl)methyl 2-amino-3-phenylpropanoate (83). Light yellow solid, yield 88%. R_f = 0.57 (10% MeOH in DCM). Mp 158–160 °C. ^{1}H NMR (400 MHz, DMSO-d_6) δ: 7.87 (s, 1H), 7.65 (d, J = 8.0 Hz, 2H), 7.36 (t, J = 8.4 Hz, 2H), 7.30–7.18 (m, 4H), 7.12 (d, J = 6.5 Hz, 1H), 6.68–6.66 (m, 1H), 5.09 (m, 2H), 4.58 (t, J = 7.7 Hz, 2H), 4.49 (s, 2H), 4.34 (d, J = 5.6 Hz, 2H), 3.60–3.57 (m, 1H), 2.84–2.76 (m, 4H). ^{13}C NMR (75 MHz, $CDCl_3$) δ: 174.15, 169.49, 146.34, 142.24, 141.93, 129.30, 128.89, 128.53, 127.76, 127.03, 125.61, 125.09, 123.15, 56.06, 52.65, 46.18, 43.10, 36.28. IR ν_{max} (neat)/cm^{-1} 3298 (NH_2) and 3070 (CH). MS (ESI), m/z: 474.8 $[M - H]^-$, 476.3 $[M + H]^+$.

(*R*)-(1-(3-(4-Trifluoromethylbenzylamino)-3-oxopropyl)-1*H*-1,2,3-triazol-4-yl)methyl pyrrolidine-2-carboxylate (84). Yellow oil, yield 89%. R_f = 0.35 (10% MeOH in DCM). ^{1}H NMR (300 MHz, $CDCl_3$) δ: 8.43 (brs, 1H), 7.56 (s, 1H), 7.40–7.21 (m, 4H), 5.23 (brs, 1H), 4.64 (m, 2H), 4.47 (s, 2H), 4.34 (d, J = 6.5 Hz, 2H), 3.78–3.64 (m, 1H), 3.32–3.21 (m, 2H), 2.87 (t, J = 8.8 Hz, 2H), 2.31–2.21 (m, 1H), 2.08–1.77 (m, 3H). ^{13}C NMR (75 MHz, $CDCl_3$) δ: 174.12, 169.72, 149.58, 137.26, 129.65, 127.78, 126.92, 125.61, 123.18, 58.16, 54.48, 46.09, 43.14, 35.51, 31.03, 29.70, 24.32. IR ν_{max} (neat)/cm^{-1} 3298 (NH_2) and 3095 (CH). MS (ESI), m/z: 426.05 $[M + H]^+$.

(*R*)-(1-(3-(4-(Trifluoromethyl)benzylamino)-3-oxopropyl)-1*H*-1,2,3-triazol-4-yl)methyl 2-amino-3-(1*H*-indol-3-yl)propanoate (85). Yellow oil, yield 85%. R_f = 0.64 (10% MeOH in DCM). ^{1}H NMR (400 MHz, $CDCl_3$) δ: 8.96–8.94 (m, 1H), 8.15 (d, J = 8.0 Hz, 1H), 8.06–8.00 (m, 3H), 7.64 (t, J = 7.2 Hz, 1H), 7.57–7.51 (m, 4H), 7.15 (t, J = 7.1 Hz, 1H), 6.99 (s, 1H), 4.97 (s, 2H), 4.65–4.59 (m, 2H), 4.43–4.38 (m, 2H), 3.51–3.48 (m, 1H), 2.96 (brs, 2H), 2.88 (brs, 2H). ^{13}C NMR (75 MHz, $CDCl_3$) δ: 175.40, 169.53, 147.34, 141.88, 136.45, 133.46, 129.99, 128.87, 127.76, 125.61, 124.54, 123.16, 121.78, 119.64, 118.74, 110.98, 109.12, 58.67, 55.89, 46.20, 43.12, 36.23, 29.68. IR ν_{max} (neat)/cm^{-1} 3284 (NH_2) and 3063 (CH). MS (ESI), m/z: 515.3 $[M + H]^+$.

(*R*)-(1-(3-(4-Trifluoromethoxybenzylamino)-3-oxopropyl)-1*H*-1,2,3-triazol-4-yl)methyl 2-amino-3-phenylpropanoate (86). Yellow oil, yield 89%. R_f = 0.57 (10% MeOH in DCM). ^{1}H NMR (300 MHz, $CDCl_3$) δ: 7.57 (s, 1H), 7.32–7.11 (m, 9H), 6.54 (brs, 1H), 5.14 (s, 2H), 4.61 (t, J = 5.8 Hz, 2H), 4.51 (s, 2H), 4.33–4.25 (m, 2H), 3.65–3.52 (m, 1H), 3.12–3.01 (m, 2H), 2.82 (t, J = 6.8 Hz, 2H). ^{13}C NMR (75 MHz, $CDCl_3$) δ: 172.87, 168.71, 157.26, 142.77, 137.56, 134.09, 130.45, 128.92, 127.87, 127.45, 126.09, 123.29, 121.56, 58.51, 54.71, 46.31, 43.71, 40.83, 35.55. IR ν_{max} (neat)/cm^{-1} 3287 (NH_2) and 3056 (CH). MS (ESI), m/z: 492.3 $[M + H]^+$.

(*R*)-(1-(3-(4-Trifluoromethoxybenzylamino)-3-oxopropyl)-1*H*-1,2,3-triazol-4-yl)methyl pyrrolidine-2-carboxylate (87). Light yellow oil, yield 89%. R_f = 0.38 (10% MeOH in DCM). ^{1}H NMR (300 MHz, $CDCl_3$) δ: 8.54 (brs, 1H), 7.89 (s, 1H), 7.67–7.43 (m, 2H), 7.31–7.23 (m, 2H), 5.20 (brs, 1H), 4.64 (t, J = 7.2 Hz, 2H), 4.54 (s, 2H), 4.29 (d, J = 6.7 Hz, 2H), 3.78–3.62 (m, 1H), 3.28–3.21 (m, 2H), 2.89 (t, J = 7.6 Hz, 2H), 2.22–2.04 (m, 2H), 1.89–1.72 (m, 2H). ^{13}C NMR (75 MHz, $CDCl_3$) δ: 173.45, 169.52, 149.23, 138.45, 129.34, 128.43, 127.89, 127.34, 122.89, 60.56, 56.45, 46.58, 43.76, 36.52, 30.93, 29.81, 24.56. IR ν_{max} (neat)/cm^{-1} 3290 (NH_2) and 3065 (CH). MS (ESI), m/z: 442.3 $[M + H]^+$.

(*R*)-(1-(3-(4-Trifluoromethoxybenzylamino)-3-oxopropyl)-1*H*-1,2,3-triazol-4-yl)methyl 2-amino-3-(1*H*-indol-3-yl)propanoate (88). Yellow oil, yield 89%. R_f = 0.62 (10% MeOH in DCM). ^{1}H NMR (300 MHz, $CDCl_3$) δ: 8.73 (s, 1H), 7.65 (d, J = 7.8 Hz, 1H), 7.47 (d, J = 7.8 Hz, 1H), 7.36–7.25 (m, 5H), 7.12–6.99 (m, 3H), 6.46 (s, 1H), 5.23–5.14 (m, 2H), 4.60–4.53 (m, 2H), 4.32 (d, J = 6.0 Hz, 2H), 3.87–3.76 (m, 1H), 3.25–3.11 (m, 2H), 2.90–2.77 (m, 2H). ^{13}C NMR (75 MHz, $CDCl_3$) δ: 174.24, 169.48, 156.24, 143.43, 137.89, 135.23, 128.56, 127.51, 127.32, 124.43, 123.29, 122.56, 121.76, 119.32, 118.67, 111.48, 109.62, 58.45, 54.76, 46.23, 43.54, 35.72, 30.35. IR ν_{max} (neat)/cm^{-1} 3294 (NH_2) and 3066 (CH). MS (ESI), m/z: 531.3 $[M + H]^+$.

Biology

***In vitro* anti-*Candida* activity.** The anticandidal assessment of title compounds (**65–88**) was performed by the broth dilution technique according to the standard protocol of NCCLS, 2012.[30] In this study, *C. albicans* ATCC 90028, *C. albicans* 10261, *C. glabrata* ATCC 90030, *C. tropicalis* ATCC 750 and FLC-sensitive/resistant clinical isolates of *C. albicans* were used for anticandidal activity assessment. Fluconazole was used as a positive control. Varying concentrations (1000 to 7.8 μg mL^{-1}) of test compounds were dispensed into a 96-well plate in Sabouraud dextrose broth medium in a final volume of 100 μL. *Candida* cells were harvested and their turbidity was assessed according to the McFarland standards. Then, 100 μL of cells (approximately 2.5 × 10^3 cells per mL) were dispensed into the 96 wells and incubated at 37 °C for 24 h. After incubation, the growth was measured turbidometrically at 600 nm using a Thermo Multiskan spectrophotometer. IC_{50} was determined as 50% inhibition of *Candida* growth and calculated by plotting a graph between the concentration ($\log_{10}$) and % inhibition.

Time kill curve study. The fungicidal or fungistatic effect of lead inhibitors **68** and **70** was determined by the time–kill curve assay according to the method reported by Jiang *et al.*[31] For standard as well as resistant strains of *C. albicans*, the cells were exposed to 60 and 120 μg mL^{-1} concentrations of **68** and **70**. Fluconazole (125 and 1000 μg mL^{-1}) was used as a positive control against standard and FLC-resistant *C. albicans*, respectively. The untreated cells were used as a negative control. All time–kill curve experiments were conducted in triplicate and the mean colony count data ($\log_{10}$ CFU mL^{-1}) were plotted as a function of time for each strain.

Proteinase and phospholipase assay. Previously identified proteinase positive standard *C. albicans* ATCC 90028 along with FLC-sensitive and resistant clinical isolates of *C. albicans* were used for this study. 1.5 mL of the 24 h old *Candida* cells were transferred into micro-centrifuge tubes and centrifuged at 3000 rpm for 5 min. The pellets obtained were washed in phosphate buffer saline (PBS) twice and centrifuged to remove the residual medium. After standardizing the suspensions

(MacFarland standard), the cells were exposed to 60 and 120 μg mL^{-1} of lead inhibitors (**68** and **70**) for 1 h. Then, 1 μL from each cell suspension treated with the test compound was plated at equidistant points on proteinase and phospholipase agar media and incubated at 37 °C for 3–4 days.[32] The formation of a transparent halo around the *Candida* colonies indicated the effect of the test compounds on extracellular enzyme secretion. Enzyme activity was measured by dividing the diameter of the colony by the diameter of the colony plus zone of clearance.[33] The experiment was performed in triplicate.

Transmission electron microscopy (TEM) analysis. The morphology of *Candida* cells was analyzed using TEM following the standard protocol.[34] Mid-log phase cells were harvested, standardized ($A_{600} \approx 0.1$) and exposed to a 120 μg mL^{-1} concentration of test inhibitors **68** and **70** for 1 h. Then, the cells were washed thrice with PBS to remove the residual medium and fixed overnight in 2.5% glutaraldehyde in phosphate/magnesium buffer (40 mM K_2HPO_4/KH_2PO_4, pH 6.5, 0.5 mM $MgCl_2$). The cells were washed twice for 15 min in 0.1 M sodium phosphate buffer (pH 6.0) and post-fixed for 2 h in 2% osmium tetroxide. Again, the cells were washed twice for 15 min in distilled water and then *en bloc* stained with 1% uranyl acetate (aqueous) for 30 min. After two further washes, the cells were dehydrated in 95% and 100% ethanol. The cells were exposed to propylene oxide for 2 × 10 min and infiltrated for 1 h in a 1 : 1 propylene/epoxy embedding material (Epon) mixture and then overnight in fresh Epon. After polymerization for 48 h at 60 °C, ultrathin sections were cut using a microtome (LeicaEM UC6) and transferred onto a copper grid. The samples were stained with uranyl acetate (saturated solution of uranyl acetate in 50% alcohol) followed by lead citrate. The samples were washed three times in Milli-Q (MQ) water and dried by touching with Whatman filter paper. The sections were examined with a Jeol (Japan) JEM-2100F transmission electron microscope at 120 kV.

Ergosterol estimation assay. The total intracellular sterols were extracted as reported earlier with slight modifications.[22] Three separate conical flasks containing 30, 60 and 120 μg mL^{-1} of compounds **68** and **70** in Sabouraud dextrose broth were inoculated with fresh cells of *C. albicans* ATCC 90028 (standard) and FLC-resistant *C. albicans*. Fluconazole (40 μg mL^{-1}) was used as a positive control while the untreated cells as a negative control for comparison. All the conical flasks were incubated at 35 °C for 16 h. After incubation, the cells were harvested at their stationary phase and the weight of the pellet was determined. The pellet was treated with 25% alcoholic potassium hydroxide (KOH) solution followed by incubation at 85 °C for 1 h. After incubation, sterol was extracted by the addition of the *n*-heptane : distilled water (1 : 3) mixture. The heptane layers were transferred into a fresh test tube, diluted five-fold in 100% ethanol and scanned spectrophotometrically between 240 and 300 nm. The presence of ergosterol and the late sterol intermediate 24(28)DHE in the extracted sample resulted in a characteristic four peak curve. The absence of detectable ergosterol in the extract was indicated as a flat line. The ergosterol content was calculated as a percentage wet weight of the cell by using the following the equation:

$$\%\text{Ergosterol} + \%24(28)\text{DHE} = [(A_{281.5}/290) \times F]/\text{pellet weight}$$

where, %24(28)DHE = $[(A_{230}/518) \times F]$/pellet weight, $A_{281.5}$ and A_{230} are absorbances at 281.5 nm and 230 nm, respectively, and F is the factor for dilution in ethanol.

Cell proliferation assay. MTT (3-(4,5-dimethyl-2-yl)-2,5-diphenyl tetrazolium bromide), Dulbecco's modified Eagle's medium (DMEM), 0.25% trypsin, and a 0.02% EDTA mixture were purchased from Hi Media (Mumbai, India). Fetal bovine serum (FBS) was obtained from Gibco (Grand Island, NY). The human embryonic kidney (HEK293) cell line was procured from the National Centre for Cell Sciences (NCCS), Pune, India. The cells were cultured and maintained as a monolayer in DMEM supplemented with 10% FBS and antibiotics (100 units per mL penicillin and 100 μg mL^{-1} streptomycin) at 37 °C under a humidified atmosphere of 5% CO_2 in T-25 flasks. The cells were sub-cultured twice in a week. A cell count of approximately 2 × 10^4 cells per well were seeded in a 96-well plate (150 μL per well) and incubated for 24 h before treatment. The cells were then treated with varying concentrations (10–600 μg mL^{-1}) of the test compounds. After 48 h of incubation at 37 °C, the exhausted serum supplemented medium was removed and serum free media (50 μL) was added into each well. After that, 20 μL per well of MTT at a concentration of 5 mg mL^{-1} in PBS was added to each well and the plates were incubated for 4 h at 37 °C. Formazan crystals, the metabolized MTT product, were solubilized in DMSO (150 μL per well) and were quantified by reading the absorbance at 570 nm after incubation of 10 min on an *iMark* Microplate Reader (Bio-Rad, Hercules, CA). All assays were performed in triplicate. Percent viability was taken as the relative absorbance of treated *versus* untreated control cells.[35]

Hemolytic assay. The hemolytic activities of the test inhibitors **68** and **70** and the conventional antifungal drug FLC were determined on human red blood cells (hRBCs).[36] Human erythrocytes from healthy individuals were collected in tubes containing EDTA as an anti-coagulant. The erythrocytes were harvested by centrifugation for 10 min at 2000 rpm and 20 °C, and washed three times in PBS. To the pellet, PBS was added to yield a 10% (v/v) erythrocytes/PBS suspension. The 10% suspension of erythrocytes was then further diluted with PBS at a 1 : 10 ratio. 100 μL of the final diluted erythrocytes was added to 100 μL of PBS having a previously determined concentration gradient (1000 to 7.8 μg mL^{-1}) of test compounds in micro-centrifuge tubes. Total hemolysis was achieved with 1% Triton X-100. The tubes were incubated for 1 h at 37 °C and then centrifuged for 10 min at 2000 rpm and at room temperature. From the supernatant fluid, 150 μL was transferred to a flat-bottomed microtiter plate (Tarson), and the absorbance was measured spectrophotometrically at

450 nm by using a Thermo Multiskan spectrophotometer. The hemolysis percentage was calculated by following the equation:

$$\%\text{Hemolysis} = \left[(A_{450}\text{ of test compound treated sample} - A_{450}\text{ of buffer treated sample})/(A_{450}\text{ of 1\% Triton X-100 treated sample} - A_{450}\text{ of buffer treated sample})\right] \times 100\%.$$

Where A_{450} is the absorbance at 450 nm.

Modeling the CYP51 like protein structure. The primary protein sequence of CYP51 was extracted from a protein database at NCBI[37] and its homologous sequence from the PDB with PDB ID-4LXJ.[38] Modeller 9.15[39] was used to generate 5 models of the *Candida* CYP51 protein using the *S. cervisiae* CYP51 protein (PDB ID-4LXJ) as a template. Structure validation of these models was performed using Procheck,[40] verified in 3D[41] and superimposed using Chimera[42] for structure comparison.

***In silico* docking.** The 3D structures of the two shortlisted compounds, **68** and **70** were drawn using Chem Draw.[43] We used model 3 for further *in silico* analysis. The computational docking method predicts the ligand–macromolecule bound states with their binding affinities using a scoring function. We have used AUTODOCK VINA 1.1.2[44] in the present study that uses Iterated Local Search Global Optimization algorithm for local minima search.[45,46] We performed *in silico* blind docking of the complete protein molecule of model 3 against the two shortlisted compounds **68** and **70**. We used ADT tools to process the protein and ligand PDBs into ADT desired format (PDBQT). Protein processing includes removal of water molecules, addition of hydrogen and charges to the protein and likewise the ligand was processed (**68** and **70**) for ADT format. The grid dimensions of X, Y and Z covering the complete model 3 of the CYP51 protein molecule was 64, 60 and 52 with 1 Å spacing. The dimensions of the centre grid box were 23.27, 15.94 and 19.74 in the case of whole CYP51 molecule blind docking. The complex with the minimum binding energy and involving more number of interactions were chosen as the basis for further interface analysis. We mapped and visualized these interacting partners in PyMol.[47] Binding affinities of both lead compounds (**68** and **70**) with the modeled CYP51 were quantitated and are represented as kcal mol^{-1}. The images were prepared using the LIGPLOT visualizing program[48] and the polar and hydrophobic contacts between them were noted down.

***In vivo* assessment of the efficacy of lead inhibitors (68 and 70) against *Galleria mellonella* larvae.** The larvae of the sixth developmental stage of *G. mellonella* were obtained from the Meal Worm Company (Sheffield, England). The larvae of *G. mellonella* were stored in wood shavings in the dark at 15 °C prior to use. The larvae that were chosen for experiments weighed 0.21 g and were used within 3–4 weeks of receipt. Ten healthy larvae were placed in sterile 9 cm Petri dishes with Whatman filter paper inserted inside. A culture of *C. albicans* was grown to the stationary phase (1–2 × 10^8 mL^{-1}) in YEPD broth at 30 °C and 200 rpm. The cells were harvested by centrifugation (2056*g* for 5 minutes on a Beckmann GS-6 bench centrifuge) washed in PBS and re-suspended in PBS at a cell density of 5 × 10^5 per 20 μL. The larvae were inoculated by injecting 20 μL through the last left pro-leg into the haemocoel using a Myjector syringe (Terumo Europe) and placed at 30 °C in the dark. One h post inoculation, the larvae were inoculated with compounds **68** and **70**, both at a concentration of 2.5 mg suspended in PBS, supplemented with 12.5% DMSO (v/v), through the last right pro-leg. The larvae injected with 20 μL of PBS supplemented with 12.5% DMSO (v/v) were used as controls. For assessment of larval viability, the larvae were gently probed with a needle and if no response was observed, the larvae were considered to be dead.

Three larvae were inoculated with 20 μL of compounds **68** and **70** solutions at concentrations of 1.25 or 2.5 mg mL^{-1}. The larvae were then incubated at 30 °C, in the dark, for 24 h. The haemocyte density in the larvae was ascertained by piercing the backs of the anterior end ('head') of the three larvae with a sterile needle and collecting the yellow haemolymph ('blood'), ensuring no white flocular material was removed – this is the fat body and will impede counting. Haemolymph was diluted to 1 in 10 in cold PBS containing 0.37% (v/v) 2-mercaptoethanol to reduce clotting and melanisation. The solution was mixed gently by pipetting. Haemocytes were counted on a haemocytometer (0.0025 mm^2, BlauBrand, Germany) and the density in the original larvae was calculated.

Five larvae of *G. mellonella* were inoculated with *C. albicans* at a density of 5 × 10^5 per 20 μl and incubated at 30 °C in the dark. 1 h post inoculation, larvae were inoculated with compounds **68** and **70** both at a concentration of 2.5 mg suspended in PBS supplemented with 12.5% DMSO (v/v). Three larvae were selected and placed in a sterile pestle with 3 mL of PBS and ground to a pulp with a mortar. The resulting homogenate was diluted with PBS and 100 μL of the sample was plated onto three YEPD-erythromycin plates (to prevent bacterial growth). The homogenate was diluted to 1/10 in PBS prior to plating. The plates were incubated at 30 °C for 24 h and the colony forming units were enumerated. The fungal load in the larvae was calculated by multiplying this figure by the relevant dilution factors.

Conclusions

In summary a novel series of 1,2,3-triazole–amino acid hybrids was prepared in an attempt to search for potent antifungal agents that can be effective against the FLC-sensitive and resistant strains of *Candida* species. Out of 24, twelve compounds (**65**, **67–71**, **73–74**, **79**, **82–83**, **85**) showed comparatively lower IC_{50} values against various standard *Candida* strains and were found to be non-cytotoxic on the HEK293 cell line up to a concentration of 200 μg mL^{-1}. Seven compounds (**67–68**, **70–71**, **73**, **79**, **82**) were selected for their inhibitory potential

against FLC sensitive and resistant clinical *C. albicans* isolates and identified two lead compounds **68** and **70** with the most potent antifungal activity against all the strains used. Time kill testing assay confirmed the fungistatic nature of the lead compounds (**68** and **70**). They also effectively inhibited the extracellular secretion of the enzymes in proteinase and phopholipase assays against FLC sensitive and resistant clinical *C. albicans* isolates. These enzymes are responsible for the fungal invasion of host tissues and immune suppression. TEM analysis showed that compounds **68** and **70** caused significant damage to *C. albicans* cells. Alterations in the cell wall structure suggests that these antifungal compounds may cause cell death resulting from inhibiting the synthetic route of fungal cell wall formation. The effect of **68** and **70** on the intracellular ergosterol content in FLC-sensitive and resistant *C. albicans* clinical strains were also examined which revealed the inhibition of ergosterol biosynthesis thereby producing an anti-*Candida* effect. An overall understanding of the interaction of the lead inhibitors **68** and **70** with the modeled *Candida* like CYP51 protein will help in knowledge based design of better leads with more potent antifungal activity. Compounds **68** and **70** not only proved to be the most potent anti-*Candida* agents in *in vitro* assays but also displayed promising *in vivo* efficacy in the *G. mellonella* larvae model. The administration of a dose of 2.5 mg mL^{-1} of **68** and **70** to the larvae did not affect the viability confirming their non-toxic behaviour. Also, no significant alteration in the haemocyte density was observed which indicated the lack of an immune response. Compound **68** caused about 50% inhibition to the larvae infected with *C. albicans* while **70** reduced 70% yeast replication *in vivo* as measured at 24 h. Our results strongly support that the lead inhibitors (**68** and **70**) provide a good starting point for lead optimization and efficacy for clinical studies.

Conflict of interest

The authors declare no competing financial interest.

Acknowledgements

Mohammad Abid gratefully acknowledges UGC, Govt. of India for the major research Project (Grant No. 41-277/2012 (SR)) and for the Raman Postdoctoral Fellowship in USA (F. No. 5-123/2016 (IC)). BA acknowledges the BSR fellowship and MI acknowledges the Non-NET fellowship support from UGC, INDIA.

Notes and references

1 B. Yao, H. Ji, Y. Cao, Y. Zhou, J. Zhu, J. Lü, Y. Li, J. Chen, C. Zheng, Y. Jiang and R. Liang, *J. Med. Chem.*, 2007, **50**, 5293–5300.
2 S. Tobudic, C. Kratzer and E. Presterl, *Mycoses*, 2012, **55**, 24–32.
3 A. H. Groll and J. Lumb, *Future Microbiol.*, 2012, **7**, 179–184.
4 CDC, *Antibiotic resistance threats in the United States*, U.S. Department of Health and Human Services, Atlanta, Georgia, 2013, pp. 63–64.
5 G. D. Brown, D. W. Denning, N. A. Gow, S. M. Levitz, M. G. Netea and T. C. White, *Sci. Transl. Med.*, 2012, **4**, 165rv13.
6 X. Cao, Z. Sun, Y. Cao, R. Wang, T. Cai, W. Chu, W. Hu and Y. Yang, *J. Med. Chem.*, 2014, **57**, 3687–3706.
7 R. A. Calderone, Introduction and historical perspectives, in *Candida and Candidiasis*, ed. R. Calderone, ASM Press, Washington, DC, 2002, pp. 15–25.
8 C. A. Kauffman, J. A. Vazquez, J. D. Sobel, H. A. Gallis, D. S. McKinsey, A. W. Karchmer, A. M. Sugar, P. K. Sharkey, G. J. Wise, R. Mangi and A. Mosher, *Clin. Infect. Dis.*, 2000, **30**, 14–18.
9 S. Silva, M. Negri, M. Henriques, R. Oliveira, D. W. Williams and J. Azeredo, *FEMS Microbiol. Rev.*, 2012, **36**, 288–305.
10 R. M. Donlan and J. W. Costerton, *Clin. Microbiol. Rev.*, 2002, **15**, 167–193.
11 W. L. Chaffin, J. L. López-Ribot, M. Casanova, D. Gozalbo and J. P. Martínez, *Microbiol. Mol. Biol. Rev.*, 1998, **62**, 130–180.
12 S. Wang, Y. Wang, W. Liu, N. Liu, Y. Zhang, G. Dong, Y. Liu, Z. Li, X. He, Z. Miao, J. Yao, J. Li, W. Zhang and C. Sheng, *ACS Med. Chem. Lett.*, 2014, **5**, 506–511.
13 R. Di Santo, A. Tafi, R. Costi, M. Botta, M. Artico, F. Corelli, M. Forte, F. Caporuscio, L. Angiolella and A. T. Palamara, *J. Med. Chem.*, 2005, **48**, 5140–5153.
14 M. A. Ator, S. J. Schmidt, J. L. Adams, R. E. Dolle, L. I. Kruse, C. L. Frey and J. M. Barone, *J. Med. Chem.*, 1992, **35**, 100–106.
15 C. Sheng, W. Zhang, H. Ji, M. Zhang, Y. Song, H. Xu, J. Zhu, Z. Miao, Q. Jiang, J. Yao, Y. Zhou, J. Zhu and J. Lü, *J. Med. Chem.*, 2006, **49**, 2512–2525.
16 K. Pawar, A. Yadav, P. Prasher, S. Mishra, B. Singh, P. Singh and S. S. Komath, *MedChemComm*, 2015, **6**, 1352–1359.
17 M. Irfan, B. Aneja, U. Yadava, S. I. Khan, N. Manzoor, C. G. Daniliuc and M. Abid, *Eur. J. Med. Chem.*, 2015, **93**, 246–254.
18 B. Aneja, M. Irfan, M. I. Hassan, P. Amresh, U. Yadava, C. G. Daniliuc, M. Zafaryab, M. M. A. Rizvi, A. Azam and M. Abid, *J. Enzyme Inhib. Med. Chem.*, 2015, 1–19.
19 M. M. Masood, V. K. Pillalamarri, M. Irfan, B. Aneja, M. A. Jairajpuri, M. Zafaryab, M. M. A. Rizvi, U. Yadava, A. Addlagatta and M. Abid, *RSC Adv.*, 2015, **5**, 34173–34183.
20 M. Schaller, C. Borelli, H. C. Korting and B. Hube, *Mycoses*, 2005, **48**, 365–377.
21 A. B. Salake, A. S. Chothe, S. S. Nilewar, M. Khilare, R. S. Meshram, A. A. Pandey and M. K. Kathiravan, *J. Chem. Biol.*, 2014, **7**, 29–35.
22 B. A. Arthington-Skaggs, D. W. Warnock and C. J. Morrison, *Antimicrob. Agents Chemother.*, 2000, **44**, 2081–2085.
23 H. Ji, W. Zhang, M. Zhang, M. Kudo, Y. Aoyama, Y. Yoshida, C. Sheng, Y. Song, S. Yang, Y. Zhou and J. Lü, *J. Med. Chem.*, 2003, **46**, 474–485.

24 K. Asai, N. Tsuchimori, K. Okonogi, J. R. Perfect, O. Gotoh and Y. Yoshida, *Antimicrob. Agents Chemother.*, 1999, **43**, 1163–1169.
25 J. Fallon, J. Kelly and K. Kavanagh, in *Host-Fungus Interactions*, Humana Press, 2012, pp. 469–485.
26 S. Zhang, J. Zou, M. Elsabahy, A. Karwa, A. Li, D. A. Moore, R. B. Dorshow and K. L. Wooley, *Chem. Sci.*, 2013, **4**, 2122–2126.
27 T. Asaba, T. Suzuki, R. Ueda, H. Tsumoto, H. Nakagawa and N. Miyata, *J. Am. Chem. Soc.*, 2009, **131**, 6989–6996.
28 R. Ramapanicker, R. Gupta, R. Megha and S. Chandrasekaran, *Int. J. Pept.*, 2011, 854952.
29 S. P. Chakrabarty, R. Ramapanicker, R. Mishra, S. Chandrasekaran and H. Balaram, *Bioorg. Med. Chem.*, 2009, **17**, 8060–8072.
30 NCCLS, Reference method for broth dilution antifungal susceptibility testing of yeasts; Approved standard M27eA2, National Committee on Clinical Laboratory Standards, Wayne, P.a., 2002, vol. **22**, pp. 8–9.
31 Z. Jiang, Y. Wang, W. Wang, S. Wang, B. Xu, G. Fan, G. Dong, Y. Liu, J. Yao, Z. Miao and W. Zhang, *Eur. J. Med. Chem.*, 2013, **64**, 16–22.
32 R. Rüchel, R. Tegeler and M. Trost, *Sabouraudia*, 1982, **20**, 233–244.
33 M. F. Price, I. D. Wilkinson and L. O. Gentry, *Sabouraudia*, 1982, **20**, 7–14.
34 A. Khan, A. Ahmad, L. A. Khan and N. Manzoor, *Res. Microbiol.*, 2014, **165**, 411–419.
35 A. Kumar, M. Zafaryab, A. Umar, M. M. A. Rizvi, H. Z. A. Ansari and S. G. Ansari, *J. Biomed. Nanotechnol.*, 2015, **11**, 1913–1926.
36 A. Khan, A. Ahmad, I. Xess, L. A. Khan and N. Manzoor, *Phytomedicine*, 2010, **17**, 921–925.
37 Protein DB NCBI.
38 H. Berman, K. Henrick, H. Nakamura and J. L. Markley, *Nucleic Acids Res.*, 2007, **35**, D301–D303.
39 B. V. Reddy and Y. N. Kaznessis, *J. Biosci.*, 2007, **32**, 929–936.
40 R. A. Laskowski, M. W. MacArthur, D. S. Moss and J. M. Thornton, *J. Appl. Crystallogr.*, 1993, **26**, 283–291.
41 D. Eisenberg, R. Lüthy and J. U. Bowie, *Methods Enzymol.*, 1997, **277**, 396–404.
42 E. F. Pettersen, T. D. Goddard, C. C. Huang, G. S. Couch, D. M. Greenblatt, E. C. Meng and T. E. Ferrin, *J. Comput. Chem.*, 2004, **25**, 1605–1612.
43 Z. Li, H. Wan, Y. Shi and P. Ouyang, *J. Chem. Inf. Comput. Sci.*, 2004, **44**, 1886–1890.
44 O. Trott and A. J. Olson, *J. Comput. Chem.*, 2010, **31**, 455–461.
45 J. Baxter, *J. Oper. Res. Soc.*, 1981, 815–819.
46 *Hybrid metaheuristics–an emerging approach to optimization*, ed. C. Blum, A. Roli and M. Sampels, Springer-Verlag, Berlin, Heidelberg, 2008.
47 W. L. DeLano, *PyMOL*, DeLano Scientific, San Carlos, CA, 700, 2002.
48 A. C. Wallace, R. A. Laskowski and J. M. Thornton, *Protein Eng.*, 1995, **8**, 127–134.